Epigenetics
Insights

ARTICLE

Open Access

https://doi.org/10.48130/epi-0025-0003
Epigenetics Insights **2025**, 18: e004

Statistical analysis of DNA methylation patterns of tumor suppressor genes in breast cancer

Shuying Sun[1*], Ashley Pritchard[2], Emma McFall[3] and Christine Tian[4]

[1] *Department of Mathematics, Texas State University, San Marcos, Texas 78666, USA*
[2] *Kansas State University, Manhattan, Kansas 66506, USA*
[3] *Brown University, Providence, Rhode Island 02912, USA*
[4] *Harvard University, Cambridge, Massachusetts 02138, USA*
* Corresponding author, E-mail: ssun@txstate.edu

Abstract

The purpose of this study was to conduct the first-ever comprehensive analysis of methylation patterns of tumor suppressor genes (TSGs) in breast cancer. The authors first identified differentially methylated (DM) sites between tumors and matched normal tissues in both Alive and Dead samples. They then analyzed co-methylation patterns related to these DM sites and reported corresponding TSGs and non-TSGs. First, tumors had more heterogeneous methylation sites than normal tissues (40% vs < 10%) in both Alive and Dead samples. Second, there were significantly more DM sites in Dead than in Alive samples. Third, as for co-methylation patterns, in normal tissues, some DM sites tended to have strong co-methylations with many CG sites. In tumor tissues, some of these strong co-methylations were lost, and some new co-methylation relationships were developed. These patterns were seen in both Alive and Dead data. Fourth, there were more co-methylation changes between normal and tumor tissues in Dead than in Alive samples. Thirty TSGs and 92 non-TSGs were identified as having notable differences between Alive and Dead data. Finally, seven TSGs were involved in many co-methylation changes between normal and tumor tissues. These seven TSGs were hub genes in different networks.

Citation: Sun S, Pritchard A, McFall E, Tian C. 2025. Statistical analysis of DNA methylation patterns of tumor suppressor genes in breast cancer. *Epigenetics Insights* 18: e004 https://doi.org/10.48130/epi-0025-0003

Introduction

Breast cancer is the second leading cause of cancer death among women[1]. Given the detrimental effects breast cancer has on an individual's health, it is imperative to diagnose breast cancer early so that prognosis can be improved. DNA methylation, an epigenetic change, has shown promise as a potential predictor of breast cancer risk. Since DNA methylation often occurs early in carcinogenesis, it can be used to possibly predict breast cancer and improve early diagnosis and overall prognosis[2]. Previous research has established that co-methylation among genes can be used as an indicator to identify candidate genes or pathways that may play a significant role in cancer development. Akulenko & Helms identified 133 genes involved in forming 187 gene pairs whose co-methylation signals were highly correlated with one another[3]. From these genes, they were able to further identify four enriched pathways. Zhang & Huang's pan-cancer analysis of DNA co-methylation patterns identified two co-methylation clusters that separate tumor samples from normal samples in 10 out of the 11 cancer types they studied[4]. These findings can lead to the discovery of potential biomarkers in various cancers, further highlighting the importance of studying DNA methylation in the context of breast cancer.

It is crucial to study the methylation patterns of significant cancer genes. Among these genes, tumor suppressor genes (TSGs) are one of the most important types for preventing breast tumor development. TSGs are involved in preventing cancer by controlling cell division, apoptosis, and metastasis. As a result, silencing of TSGs can result in cancer[5,6]. One way for TSGs to become silenced is through epigenetic alterations such as methylation[7]. Previous studies have been performed to examine specific tumor suppressor genes and their methylation patterns across multiple cancer types[8−11]. However, to the author's best knowledge, a comprehensive analysis of different methylation patterns for all available TSGs has not yet been conducted for breast cancer. The purpose of this study was, therefore, to provide the first-ever comprehensive analysis of methylation patterns for TSGs in breast cancer.

In this study, the authors used publicly available breast cancer methylation data from The Cancer Genome Atlas (TCGA) database[12]. They analyzed the overall methylation patterns using the distribution of methylation states as defined by Tian et al.[13]. They then identified differentially methylated (DM) CG sites and associated genes. They also conducted thorough analyses of the co-methylation patterns between DM sites and all CG sites. Finally, they identified and analyzed genes with various co-methylation changes.

Materials and methods

Data

Data 1: breast cancer methylation signals

To study the methylation patterns of tumor suppressor genes and their associated CG sites, the authors used publicly available data from 53 living and 32 deceased breast cancer patients from TCGA. These datasets will be referred to as 53-Alive and 32-Dead samples throughout the rest of this paper. The Illumina human methylation 450K array data for 53-Alive and 32-Dead samples were used, including the datasets of tumor tissues and adjacent solid normal (or matched normal) tissues (i.e., Alive-Tumor, Alive-Normal, Dead-Tumor, and Dead-Normal data). The vital statuses (Alive or Dead) of all samples were determined according to the classifications provided through the TCGA. The authors will explain the reasons for choosing patients with vital statuses and matched normal (or paired) tissues in the Discussion.

Each Illumina dataset contains the beta-value (β) methylation signals of 485,577 CG sites. These beta-values range from 0 (no methylation) to 1 (full methylation). M-values are the transformation of beta methylation signals at each CG site, i.e., M = $\log_2(\beta/(1-\beta))$. Methylation signals were processed by removing CG sites that were not useful for further analysis. After processing, 391,459 CG sites were left for each sample to carry out further analyses. The processing steps are listed below.

(1) 8,233 CG sites were removed when the start position and the end position were the same. Of these sites, about 5,120 were control sites, and the remaining 3,113 sites were either single nucleotide polymorphisms or non-CG sites.

(2) 397 CG sites were removed because they were located on the Y chromosome.

(3) There were 21 duplicated CG sites with identical positions. The second of each duplication was removed.

(4) 85,467 CG sites were removed because they had NA for all samples in all four datasets (Alive Normal, Alive Tumor, Dead Normal, and Dead Tumor).

Data 2: tumor suppressor genes and associated CG sites

To study the methylation patterns of tumor suppressor genes, the 1,217 TSGs identified by Zhao et al. (i.e., TSGene 2.0)[14] were used. These genes were reported as playing the role of tumor suppressor genes in various previous studies[14]. 1,186 of these genes had at least one CG site associated with each of them. In total, 25,977 unique CG sites were associated with all TSGs. The term 'unique CG sites' meant that CG sites associated with two or more genes were only counted once. The authors also used 3,804 housekeeping (HK) genes identified by Eisenberg & Levanon[15] as a reference to study TSGs' overall methylation distribution. 3,746 of these HK genes had at least one CG site associated with each of them. In total, 67,299 unique CG sites were associated with these HK genes.

Statistical analysis

Analysis 1: methylation distribution

For every CG site in each dataset, a methylation state was assigned to be 'Low (L)', 'High (H)', 'Low-Median (LM)', 'High-Median (HM)', 'Median (M)', or 'Rest (R)' based on beta-value methylation signals, as defined by Tian et al.[13]. Figure 1 of Tian et al.[13] can be useful to visualize the definitions of methylation states. A methylation state of 'L' meant that all samples' methylation levels of the specific CG site were below 0.2. 'H' indicated all samples' methylation levels were above 0.8, and 'M' was defined if all samples' methylation levels were between 0.2 and 0.8. If a CG site did not meet any of these definitions, it was assigned to belong to either 'LM' or 'HM', where 'LM' indicated all samples had a methylation level below 0.6, and 'HM' meant all samples had a methylation level above 0.4. If a CG site did not belong to any of these categories, it was assigned a methylation state of 'R', which refers to a site with heterogeneous methylation levels.

Analysis 2: differential methylation (DM)

To identify DM sites, tumor and matched normal tissues were compared by conducting paired T-tests at each CG site using M-values, which are more statistically valid than beta-values when conducting differential analysis[16]. The mean difference between tumor and normal methylation signals at each CG site was calculated using the original beta-values. A CG site was classified as a DM site if the T-test p-value was < 0.05 and the beta |mean difference|

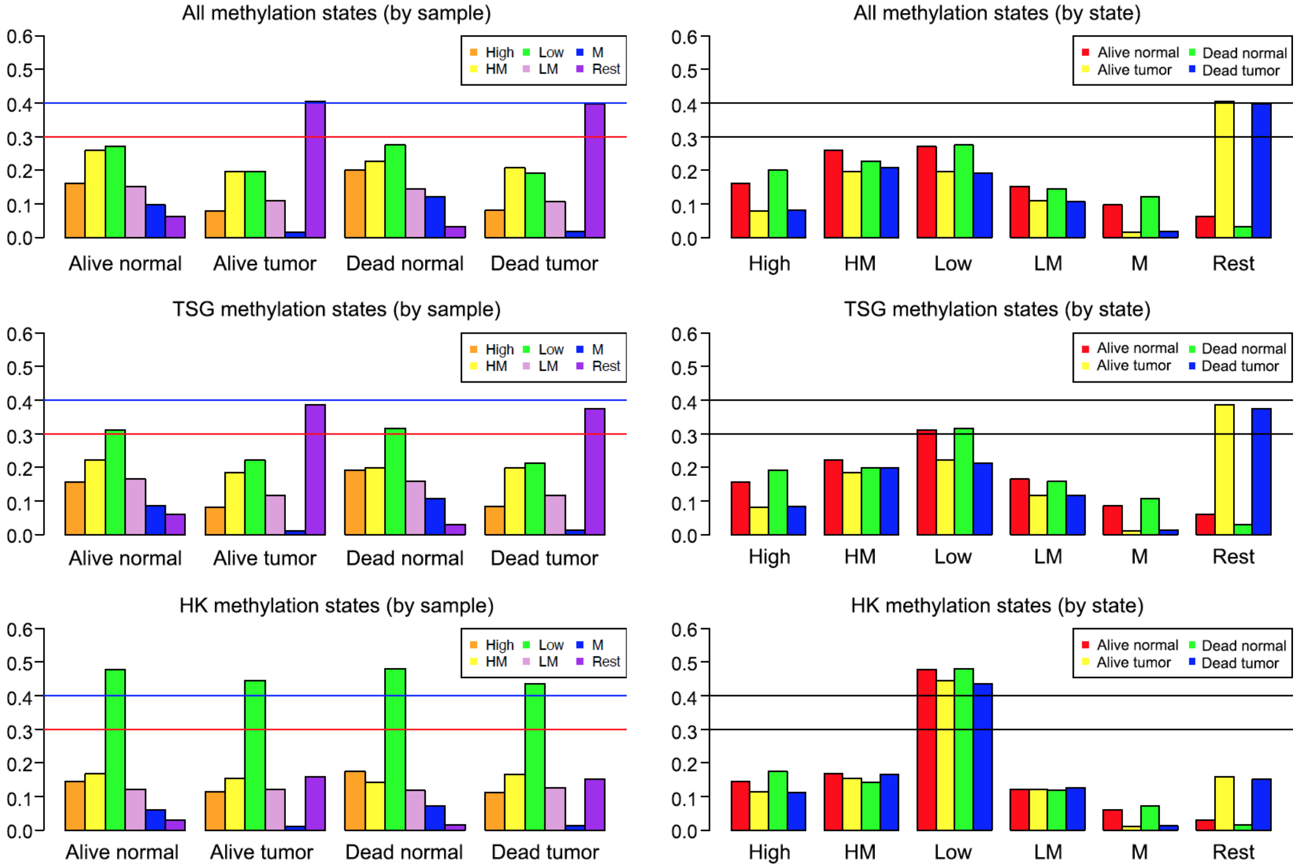

Fig. 1 Methylation states of various breast cancer samples. The vertical axis is proportion (or percentage, e.g., 0.6 means 60%). The left three plots were generated based on samples: Alive Normal, Alive Tumor, Dead Normal, and Dead Tumor. The right three plots were made based on methylation states: High, High-Median (HM), Low, Low-Median (LM), Median (M), and Rest. Two horizontal lines were drawn at 30% and 40% (i.e., 0.3 and 0.4) to make it easy to compare different samples and states.

was ≥ 0.2. This was done separately for both the 53-Alive and 32-Dead datasets.

Analysis 3: co-methylation

The authors studied the co-methylation patterns by comparing the correlation between each DM site and 391,459 CG sites for different DM categories. They started by categorizing DM sites of TSG genes into three groups based on the overlap between Alive and Dead data: alive-only DM (sites that are only DM in the Alive data), dead-only DM (sites that are only DM in the Dead data), and overlap DM (sites that are DM in both Alive and Dead data). For each of these categories, the correlation was calculated between each DM site and all CG sites using Spearman correlation coefficients. For each DM site, the total number of CG sites that were highly correlated with it was counted. Using the count per DM site and other metrics (e.g., an 8 × 8 matrix detailed later), the co-methylation patterns were compared between normal and tumor tissues as well as between Alive and Dead samples. Different co-methylation changes were identified, and corresponding genes associated with these changes were then analyzed.

Results

Methylation states

The overall methylation distribution was studied using methylation states defined in the Methods. Separate bar plots were made to illustrate the distribution by both methylation states and samples for all CG sites, TSG CG sites, and HK CG sites, see Fig. 1. This figure shows the following patterns. First, when comparing based on methylation states (see the top two plots on the right panel), TSG sites and all CG sites had a very similar distribution. The main difference between the two groups was the percentages of 'High-Median' and 'Low', as the 'Low' state had a higher percentage (slightly above 30%) in the TSG plot. Second, the methylation states of Alive Tumor and Dead Tumor were dominated by CG sites classified as 'Rest' (around 40%) in both TSG sites and all CG sites (see the two tall bars above 'Rest' at the right side of the right panels of Fig. 1). This means that the methylation signals of these CG sites have more variation in tumors than in normal tissues (40% vs < 10%). This makes sense considering the heterogeneous nature of tumor tissues. Third, CG sites classified as 'Median' (with methylation signals ranging from 0.2 to 0.8) were much fewer in tumors (far less than 10%) than in normal tissues (at least 10%). That is, normal tissues' partial methylation (i.e., 'Median') patterns were lost or removed in tumor tissues. Finally, there were noticeable differences between the methylation states of the TSG and HK CG sites (second and third panels of Fig. 1). For the TSG sites, the most prevalent methylation state in the Alive Normal and Dead Normal datasets was 'Low' (see green bars on the left panel's middle plot), meaning that the methylation signals across these CG sites are generally low or unmethylated in normal tissues. In the Alive Tumor and Dead Tumor datasets, however, CG sites that were defined as the 'Rest' state made up almost 40% of the TSG sites (see purple bars on the left panel's middle plot). In the HK data, however, over 40% of all four datasets were made up of 'Low' methylation states. That is, for HK CG sites, more than 40% of them remained unmethylated in both Alive and Dead patients' normal and tumor tissues. This shows that most HK CG sites' methylation patterns are relatively stable except for a small percentage of sites that have changed to be more heterogeneous (i.e., the 'Rest' state).

DM patterns

DM CG sites were identified by performing paired T-tests using M-values. A CG site was identified as a DM site if its *p*-value was < 0.05 and its absolute beta-value mean difference was ≥ 0.2. DM sites are summarized in Table 1. This table shows that Dead samples tended to have more DM sites than Alive samples when analyzing all 391,459 CG sites (8.68% vs 6.94%) and all TSG sites (9.34% vs 7.55%). The difference was statistically significant, see p-values shown in the last column of Table 1. As shown in Fig. 2, DM CG sites were then split into three different categories as defined in the previous section: alive-only DM, dead-only DM, and overlap DM. There were 230 alive-only DM sites, 694 dead-only DM sites, and 1,731 overlap DM sites, as shown in Fig. 2.

Unique genes that were associated with DM sites were then found and organized into three groups: 162 genes for alive-only DM sites, 483 genes for overlap DM sites, and 310 genes for dead-only DM sites. As genes can consist of multiple DM sites and a single DM site can be associated with multiple genes, the gene lists for the three DM groups are not mutually exclusive. A shared or common gene between two groups refers to a gene that has at least one DM site in both groups. The shared or common genes between each combination of two DM groups were identified, and the percentage of shared genes from each individual gene list was calculated. One hundred and sixteen genes were shared between alive-only DM and overlap DM (71.6% of Alive and 24% of overlap), 67 genes were shared between alive-only DM and dead-only DM (41.4% of Alive

Table 1. Summary of DM sites and percentages between normal and tumor tissues.

Samples	DM sites (count)	DM rates	*p*-value
Alive (for all 391,459 CG sites)	27,160	6.94%	2.2e-16
Dead (for all 391,459 CG sites)	33,974	8.68%	(Compare: 6.94% vs 8.68%)
Alive (for all 25,977 TSG CG sites)	1,961	7.55%	2.746e-13
Dead (for all 25,977 TSG CG sites)	2,425	9.34%	(Compare: 7.55% vs 9.34%)

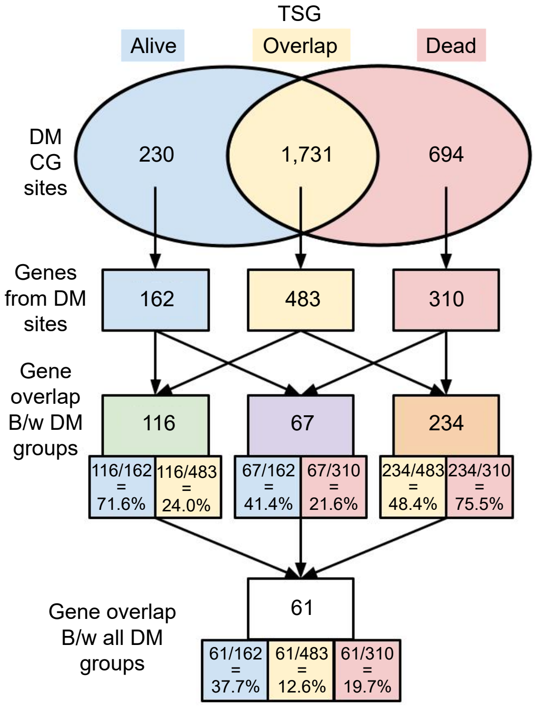

Fig. 2 Numbers of DM sites and associated genes. DM sites were identified between tumor and normal tissues in both 53-Alive and 32-Dead data. DM sites and corresponding genes associated with DM sites in each group were identified, i.e., alive-only, dead-only, and overlap in both Alive and Dead samples.

and 21.6% of Dead), and 234 genes were shared between dead-only DM and overlap DM (48.4% of overlap and 75.5% of Dead). Finally, 61 genes were common in all three DM groups (alive-only DM, dead-only DM, and overlap DM). When studying the number of CG sites on these genes, the authors found that the median and mean number of CG sites in these 61 common TSGs were 38 and 59 respectively. However, the median and mean number of CG sites in all TSGs were only 17 and 22 respectively. The 61 shared or common genes had more CG sites, indicating that these genes could be relatively long. These CG sites may have different functions or play different roles due to promoter usage. To have a concise summary, the authors focused on showing the DM results here, and some terms used above will be explained in more detail in the Discussion.

Co-methylation

Co-methylation analysis part 1: high correlation counts

To study the co-methylation patterns between DM sites and all CG sites, Spearman correlation coefficients between each DM site and all the 391,459 CG sites were calculated for each of the four datasets: 53 Alive-Tumor, 53 Alive-Normal, 32 Dead-Tumor, and 32 Dead-Normal. There were three categories for the DM sites: alive-only, dead-only, and overlap. In total, 12 different correlation matrices were calculated because there were three DM categories and four types of samples. The CG pairs with absolute correlation coefficients ≥ 0.8 were then further analyzed. These CG pairs were considered highly correlated sites. For each DM CG site, the following four numbers were counted: the number of CG sites that were highly positively correlated with it, the number of CG sites that were highly negatively correlated with it, the number of highly correlated CG sites that were on the same chromosome, and the number of highly correlated CG sites that were on different chromosomes. The authors then compared the co-methylation patterns between normal and tumor tissues as well as between Alive and Dead samples using different figures and tables.

The first four columns of Table 2 show the total number and proportion of highly co-methylated sites for each of the three DM categories (overlap, alive-only, and dead-only) for both 53-Alive and 32-Dead breast cancer patients. The last four columns of Table 2 show the total number and proportion of highly co-methylated pairs that were composed of sites on the same or different chromosomes, positively co-methylated, or negatively co-methylated. To see the patterns, the total number of highly correlated sites was plotted, see Fig. 3. Table 2 and Fig. 3 show that normal tissues had more highly co-methylated pairs than tumor tissues (the green bars are taller than the red bars), and Alive Normal had more highly co-methylated pairs than Dead Normal (two of the three left green bars are taller than the corresponding two of the three right green bars). However, in tumor tissues, there were more highly correlated pairs in Dead Tumor than in Alive Tumor (at least two of the three right red bars are taller than two left red bars). For each combination of DM category and sample type, there were more positive than negative co-methylations (≥ 80% vs ≤ 20%) and more co-methylations on different chromosomes than on the same chromosome (> 85% vs < 15%). These differences may indicate that co-methylation plays a critical role in cancer development.

Using statistical tests, the following samples were then further compared: 'normal vs tumor' and 'Alive vs Dead' for the proportions on the same (or different) chromosome and with positive (or negative) correlation. This comparison was done for the three groups of DM sites: alive-only DM, dead-only DM, and overlap DM, separately. The test results are listed in Table 3. Only the test p-values of comparing Alive-Normal with Dead-Normal (for dead-only DM and overlap DM sites) were > 0.05 (0.64 and 0.11, respectively). All the other test results were statistically significant with extremely small p-values. In many rows, the percentage differences were at least 3%. For the rows with a percentage difference < 3%, if they still had small p-values in the proportion tests, it could be due to the impact of large counts. A percentage difference of > 5% was considered as biologically significant and meaningful. Figure 4 shows that the co-methylation patterns of the three DM groups and various samples (tumor vs normal, Alive vs Dead) were very different. For example, Fig. 4's top left plot shows that the red bars (for tumors) were taller than the green bars (for normal tissues). This means that tumor tissues tend to have larger percentages of highly correlated sites on the same chromosome than the normal tissues, although the counts are not as large as the normal ones. Figure 4's top left plot shows that the percentage difference between normal and tumor was more obvious in Alive than in Dead samples. Figure 4's bottom right plot shows two (out of three) blue bars (for Alive) were taller than two corresponding black bars (for Dead). This means that there were notably greater counts and percentages of highly negative co-methylation pairs in Alive samples than in Dead samples. All the above differences suggest that differential methylation leads to the change of co-methylation in various samples.

Although Table 2 and Fig. 3 show the total number (i.e., sum) of highly correlated pairs, they do not show the overall distribution for the co-methylation patterns of all DM sites. To thoroughly compare the co-methylation patterns of different datasets (i.e., normal vs tumor, Alive vs Dead), the authors counted the number of highly correlated (with correlation |r| ≥ 0.8) partners (CG sites) per DM site in each dataset. They then drew the density plots for the counts of all DM CG sites in Alive Normal, Alive Tumor, Dead Normal, and Dead Tumor data, as shown in Fig. 5. This figure shows the distribution of these counts. For the three types of DM sites, different line types were used: solid lines for overlap DM, dashed lines for alive-only DM, and dashed-dotted lines for dead-only DM. Because the

Table 2. Highly co-methylated pairs on the same and different chromosomes and with positive and negative correlations.

DM sites	Samples	Total pairs	High.cor (%)	Same.chr (%)	Diff.chr (%)	Neg.cor (%)	Pos.cor (%)
Overlap DM (1731)	Alive.Normal	676116483	1108956 (0.164%)	65337 (5.89%)	1043619 (94.11%)	173580 (15.65%)	935376 (84.35%)
	Alive.Tumor	676116483	61217 (0.00905%)	9068 (14.81%)	52149 (85.19%)	5368 (8.77%)	55849 (91.23%)
	Dead.Normal	676116483	828833 (0.1226%)	48966 (5.91%)	779867 (94.09%)	50911 (6.14%)	777922 (93.86%)
	Dead.Tumor	676116483	343043 (0.0507%)	27970 (8.15%)	315073 (91.85%)	27812 (8.11%)	315231 (91.89%)
Alive-only DM (230)	Alive.Normal	90009005	126721 (0.1408%)	8728 (6.89%)	117993 (93.11%)	7618 (6.01%)	119103 (93.99%)
	Alive.Tumor	90009005	5760 (0.0064%)	859 (14.91%)	4901 (85.09%)	716 (12.43%)	5044 (87.57%)
	Dead.Normal	90009005	186396 (0.2071%)	11456 (6.15%)	174940 (93.85%)	5734 (3.08%)	180662 (96.92%)
	Dead.Tumor	90009005	16785 (0.0186%)	1552 (9.25%)	15233 (90.75%)	1102 (6.57%)	15683 (93.43%)
Dead-only DM (694)	Alive.Normal	271431381	973059 (0.3585%)	62739 (6.45%)	910320 (93.55%)	194705 (20.01%)	778354 (79.99%)
	Alive.Tumor	271431381	23288 (0.00858%)	3291 (14.13%)	19997 (85.87%)	3636 (15.61%)	19652 (84.39%)
	Dead.Normal	271431381	502902 (0.1853%)	32766 (6.52%)	470136 (93.48%)	32206 (6.40%)	470696 (93.60%)
	Dead.Tumor	271431381	124846 (0.046%)	10087 (8.08%)	114759 (91.92%)	9638 (7.72%)	115208 (92.28%)

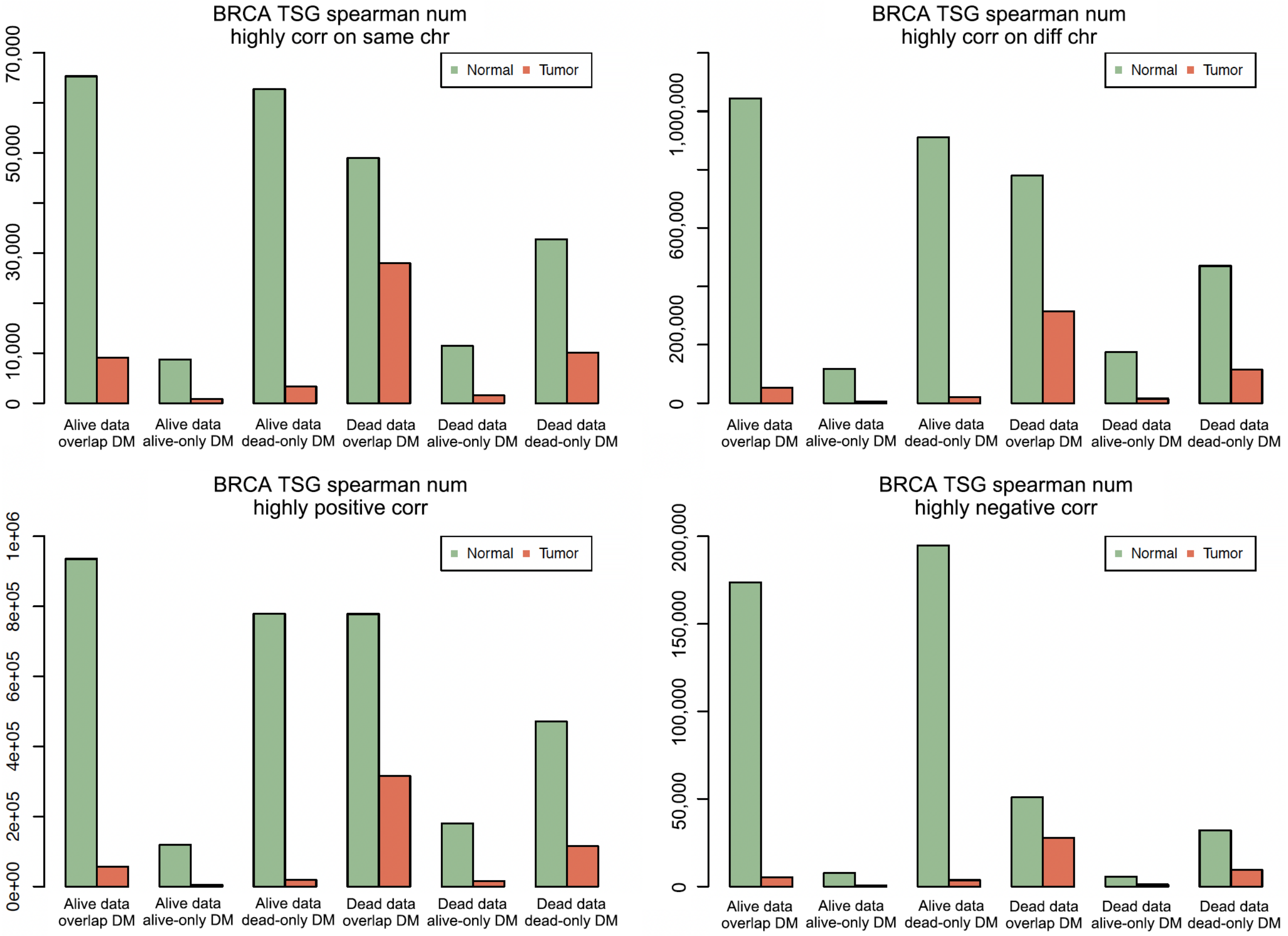

Fig. 3 The total number of highly correlated pairs in different groups. BRCA means breast cancer. In each of the four plots, the first three bar clusters are for 'Alive data, Overlap DM', 'Alive Data, Alive-only DM', and 'Alive Data, Dead-only DM', and the last three bar clusters are for 'Dead Data, Overlap DM', 'Dead Data, Alive-only DM', and 'Dead Data, Dead-only DM'.

Table 3. Proportion tests for highly co-methylated pairs of different groups.

Alive vs Dead	Same.Chr *p*-value	Same.Chr (%)	Neg.Cor *p*-value	Neg.Cor (%)
Alive Normal vs Dead Normal – Overlap DM	0.64079	5.89% vs 5.91%	0.00	15.65% vs 6.14%
Alive Tumor vs Dead Tumor – Overlap DM	0.00	14.81% vs 8.15%	4.16E-08	8.77% vs 8.11%
Alive Normal vs Dead Normal – Alive-only DM	1.17E-16	6.89% vs 6.15%	0	6.01% vs 3.08%
Alive Tumor vs Dead Tumor – Alive-only DM	4.34E-33	14.91% vs 9.25%	5.17E-45	12.43% vs 6.57%
Alive Normal vs Dead Normal – Dead-only DM	0.11344	6.45% vs 6.52%	0.00	20.01% vs 6.4%
Alive Tumor vs Dead Tumor – Dead-only DM	3.71E-192	14.13% vs 8.08%	0.00	15.61% vs 7.72%
Normal vs Tumor	Same.Chr *p*-value	Same.Chr (%)	Neg.Cor *p*-value	Neg.Cor (%)
Alive Normal vs Alive Tumor – Overlap DM	0.00	5.89% vs 14.81%	0.00	15.65% vs 8.77%
Dead Normal vs Dead Tumor – Overlap DM	0.00	5.91% vs 8.15%	0.00	6.14% vs 8.11%
Alive Normal vs Alive Tumor – Alive-only DM	0.00	6.89% vs 14.91%	0.00	6.01% vs 12.43%
Dead Normal vs Dead Tumor – Alive-only DM	1.52E-55	6.15% vs 9.25%	3.57E-127	3.08% vs 6.57%
Alive Normal vs Alive Tumor -- Dead-only DM	0.00	6.45% vs 14.13%	7.42E-62	20.01% vs 15.61%
Dead Normal vs Dead Tumor -- Dead-only DM	1.32E-85	6.52% vs 8.08%	1.90E-62	6.4% vs 7.72%

counts were extremely large for some CG sites and the distributions were very skewed, the root 4 transformation was used to show a clear pattern. Below is a summary of the key patterns of Fig. 5.

First, the top left plot shows the comparison of Alive Normal with Dead Normal (i.e., green vs blue lines). There is a peak around 0 in the Alive Normal (green lines) but not in Dead Normal (blue lines). That is, a larger number of CG sites in Alive Normal than in Dead Normal were not highly correlated with other sites. However, some CG sites were more highly correlated with many sites in Alive Normal (long green tails) than in Dead Normal (no long blue tails). Second, the top right plot shows the comparison of Alive Tumor vs Dead Tumor (i.e., red vs black lines). This plot shows the Alive Tumor had a much smaller number of highly correlated sites than the Dead Tumor (see the two red peaks near 0). On the other hand, the Dead Tumor samples had more CG sites with a high number of correlated partners (black lines). Third, the bottom left plot shows the comparison of normal and tumor tissues in the Alive data (i.e., Alive Normal vs Alive Tumor). It shows that tumor tissues had a larger number of CG sites not highly co-methylated with others (see the two tall red peaks near 0, which were much taller than the green peak around 0). Again, normal tissues had some CG sites highly co-methylated with many CG sites (see the long green tail at the right end). Fourth, the bottom

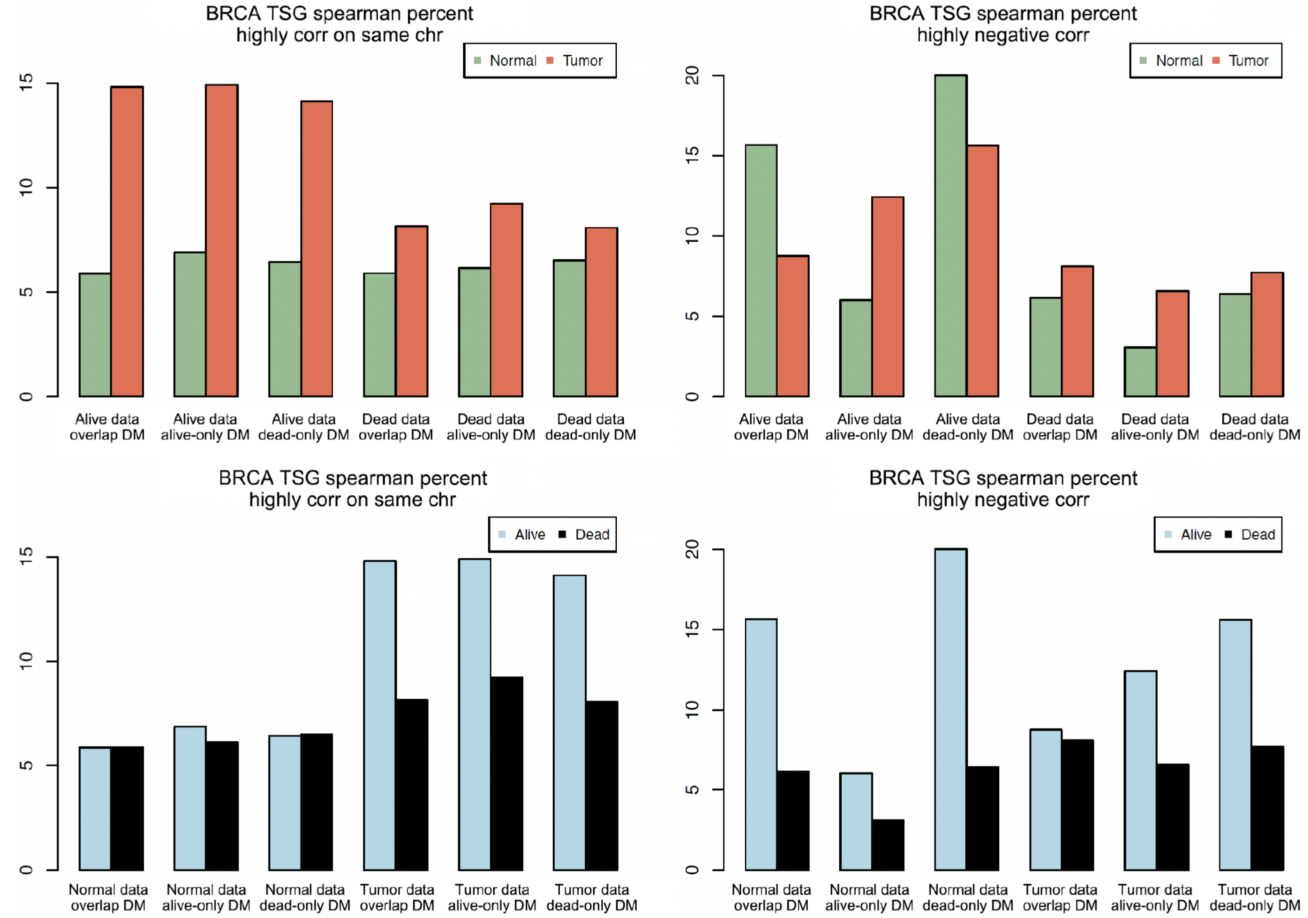

Fig. 4 Bar plots of highly correlated pairs on the same chromosome and with negative correlation. The vertical axis is the percentage (e.g., 15 means 15%).

right plot shows the comparison of normal and tumor tissues in the Dead data (i.e., Dead Normal vs Dead Tumor). This plot shows that Dead Tumor samples had more CG sites with certain correlations, but the correlations were not that strong (see the taller black lines between 0 and 5 on the left side). However, Dead Normal samples had more CG sites with strong co-methylations (see the longer blue tails at the right end). Finally, when comparing the three types of lines (solid, dashed, and dashed-dotted), their differences were much less notable than the differences between the two different colors (e.g., Alive Normal green lines vs Dead Normal blue lines). This meant that the co-methylation differences among the three types of DM sites (i.e., different types of lines) were less obvious than the differences between various samples (i.e., lines of different colors).

In summary, in normal tissues, some CG sites tended to be highly co-methylated with many other CG sites. In tumor tissues, some of these co-methylations were lost, and some new co-methylation relationships were developed. These patterns can be seen in both Alive and Dead samples. Meanwhile, the Alive and Dead samples have different co-methylation patterns. The above patterns may indicate that genes tend to maintain certain functions and interactions through co-methylation in normal tissues or in the early stage of cancers (as shown in Alive samples). However, with differential methylation, these co-methylation patterns were lost or weakened in tumor tissues or in the later stage of cancers (as shown in Dead samples).

Co-methylation analysis part 2: investigating co-methylation changes based on 8 × 8 matrices

Following previous examples[17,18], the authors calculated several 8 × 8 matrices as explained below. These matrices show in detail how co-methylation patterns of DM sites changed from normal to tumor tissues in both Alive and Dead samples. For both normal and tumor data, the correlation coefficient values were divided into eight intervals: [−1, −0.75), [−0.75, −0.5), [−0.5, −0.25), [−0.25, 0), [0, 0.25), [0.25, 0.5), [0.5, 0.75), and [0.75, 1). Each CG pair in the TSG correlation matrix was mapped to its corresponding category. For example, if a CG pair had a correlation coefficient of 0.4 in the normal tissue and 0.8 in the tumor tissue, it would be counted in the cell with the row name normal [0.25, 0.5) and column name tumor [0.75, 1). For both Alive and Dead samples, 8 × 8 matrices were calculated for each of the three DM categories: alive-only DM, dead-only DM, and overlap DM. That is, in total, there were six of these 8 × 8 correlation matrices. Figure 5 shows that the co-methylation differences among the three types of DM sites were less notable than the differences among various samples (tumor vs normal, Alive vs Dead samples). Therefore, to save some space, only two of these 8 × 8 matrices calculated based on the overlap DM sites were shown in the main text, see Table 4. Each number in the 8 × 8 matrix was a count. The percentage of CG sites for each combination was the count divided by the total number of CG sites in a specific row of the normal correlation range. For example, the count in the first cell was 4,297 (0.757%), which meant 4,297 CG pairs (i.e., 0.757% of the total pairs) had correlation coefficients in the range of [−1, 0.75) in the Alive Normal data, and they remained in [−1, 0.75) in the Alive Tumor data.

To compare the 53-Alive and 32-Dead samples' co-methylation changes between normal and tumor tissues, the authors calculated the percentage differences between corresponding Dead and Alive intervals, '% dead − % alive', for each DM category: alive-only, dead-only, and overlap. They then plotted heatmaps for these three '%

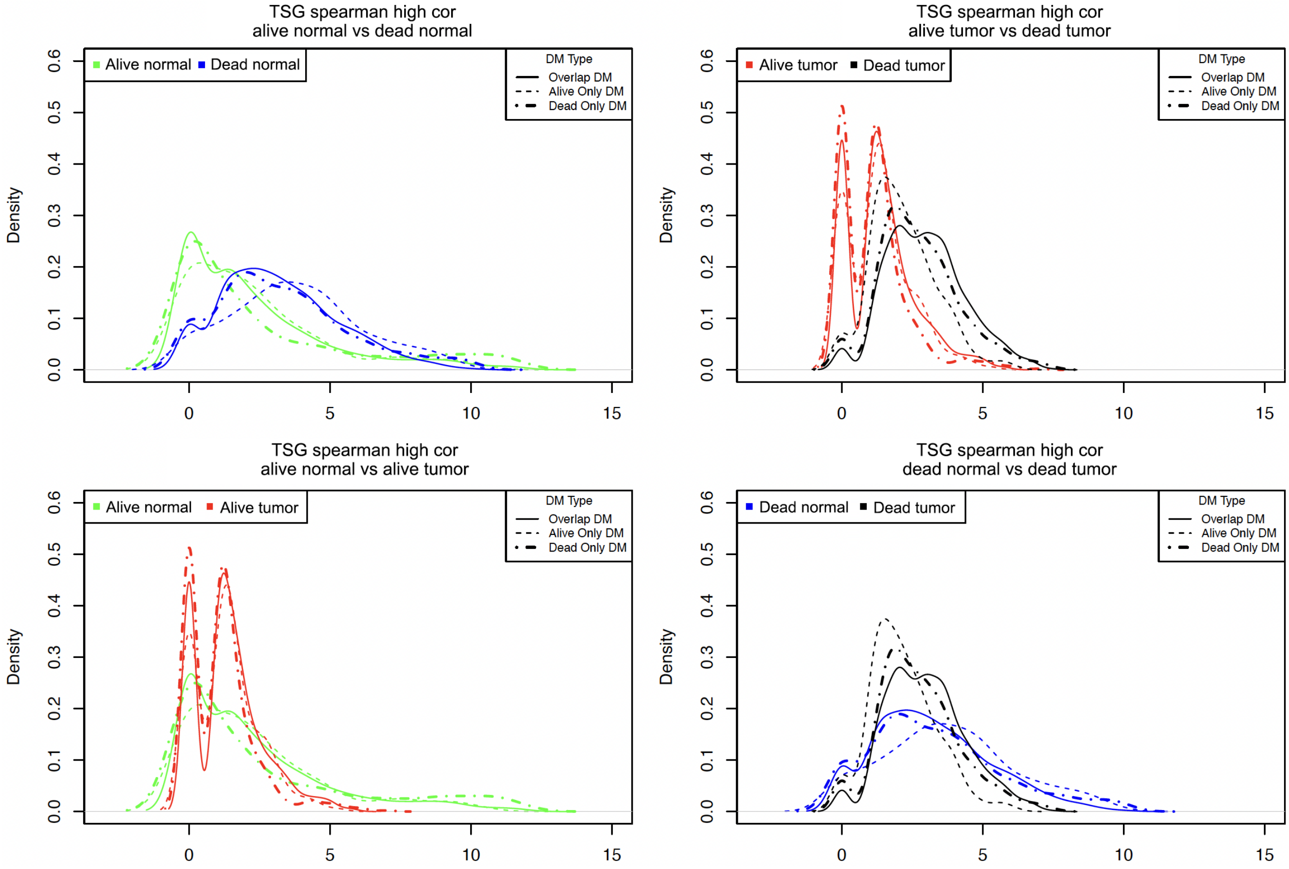

Fig. 5 Density plots for the number of highly correlated sites per DM site in different samples. Note, the count of the highly correlated partners that each DM site had was calculated and then the root 4 transformation of each count was used to generate the above density plots.

dead – % alive' matrices, as shown in Fig. 6. For the three heatmaps, there are a few striking patterns. First, the left heatmap (for alive-only DM) had a lighter overall color. However, the middle and right heatmaps had a much darker red color. This means that the dead-only DM (middle) and the overall DM (right) had a higher percentage of change than the alive-only DM (left). Second, there were darker red and blue colors in the middle rows (i.e., around the [–0.5, 0.5) intervals) of the three heatmaps. These darker colors represented larger '% dead - % alive' differences. That is, the differences in percentages were greatest in the tumor [–0.5, 0.5) intervals. This means that many CG pairs had strong correlations in the normal tissues, but they lost those strong correlations in the tumor tissues. Third, this graph shows two dark red squares on the left side of the right heatmap (for overlap DM). These dark squares meant that the largest percentage of change between Alive and Dead data was from highly negative correlations [–1, –0.75) in normal data to 'sleeping' correlations in tumor data. Note, 'sleeping' meant no/low correlation in the range of –0.5 to 0.5. The above pattern-changes show that when comparing Dead and Alive samples, there were more co-methylation changes between normal and tumor tissues in Dead samples than in Alive samples. This difference may indicate that co-methylation plays a key role in cancer development. The change of the methylation levels (i.e., differential methylation) led to the change of co-methylation in various samples and at different cancer stages.

To see the patterns of normal to tumor co-methylation changes, the 8 × 8 matrices were further condensed into 4 × 4 matrices that contained the following four intervals: [–1, 0.5), [–0.5, 0), [0, 0.5), [0.5, 1). Essentially, the authors combined the first two rows and columns, the middle four rows and columns, and the bottom two rows and columns of the 8 × 8 matrices. To modify the 8 × 8 matrices, they took the sum of the raw counts for each corresponding interval and then divided that sum by the total sum of the four rows/columns involved. This gave the percentage of CG pairs in each cell.

Bar plots were created to show the distribution of tumor correlation coefficients for each level of normal correlation, see Fig. 7. This figure shows the co-methylation change from normal to tumor based on the 4 × 4 matrix. These bar plots show that for all DM groups and all normal correlation levels, tumor [–0.5, 0) and tumor [0, 0.5) intervals were the most frequent correlation levels (see the orange and light-green bars). Additionally, for normal [–1, –0.5) and normal [–0.5, 0) intervals (i.e., the top two plots), all DM groups had a higher count in Alive than Dead samples (that is, left bar-clusters were taller than the right bar-clusters). However, for normal [0, 0.5) interval (i.e., the bottom left plot), Alive and Dead data had very similar frequencies, while for normal [0.5, 1) interval (i.e., the bottom right plot), Dead was more frequent than Alive (that is, the bar-clusters of Dead samples were taller than the ones of Alive samples). In all intervals except for the normal [–1, –0.5) interval (i.e., in the top right plot and the bottom two plots), most CG sites tended to fall into the tumor [0, 0.5) interval (i.e., the light-green bars tended to be taller than other bars). As for the normal [–1, –0.5) interval (i.e., the top left plot), most CG sites tended to fall into the tumor [–0.5, 0) interval (orange bars). Within each of the four plots, the overall pattern/distribution of the CG pair intervals was similar among the three different DM types (alive-only DM, dead-only DM, and overlap DM). The above summary shows that the strong negative and positive correlations in the normal tissues tended to be weakened or removed in the tumor tissues (see the top left and bottom right plots). Normal tissues' weak

Table 4. Two 8 × 8 matrices showing co-methylation changes between normal and tumor tissues.

Normal	Eight correlation intervals for tumor tissues (Overlap DM sites)							
Alive	T[−1, −0.75)	T[−0.75, −0.5)	T[−0.5, −0.25)	T[−0.25, 0)	T[0, 0.25)	T[0.25, 0.5)	T[0.5, 0.75)	T[0.75, 1)
N[−1, −0.75)	4297	73818	182298	201921	88579	16019	785	4
	0.7569%	**13.0025%**	**32.1105%**	**35.5669%**	**15.6026%**	**2.8216%**	**0.1383%**	**0.0007%**
N[−0.75, −0.5)	9387	446831	2224635	4629139	3733207	1167473	96376	496
	0.0763%	**3.6305%**	**18.0754%**	**37.6122%**	**30.3327%**	**9.4858%**	**0.7831%**	**0.0040%**
N[−0.5, −0.25)	6650	564390	6011579	24309202	26269230	7781659	605428	4656
	0.0101%	**0.8610%**	**9.1706%**	**37.0834%**	**40.0734%**	**11.8708%**	**0.9236%**	**0.0071%**
N[−0.25, 0)	3867	526811	10131385	62857780	86421033	26476788	1905978	15584
	0.0021%	**0.2797%**	**5.3793%**	**33.3748%**	**45.8858%**	**14.0580%**	**1.0120%**	**0.0083%**
N[0, 0.25)	2414	350385	8278526	66488860	1.20E+08	47972035	4210138	39078
	0.0010%	**0.1415%**	**3.3427%**	**26.8471%**	**48.5817%**	**19.3703%**	**1.7000%**	**0.0158%**
N[0.25, 0.5)	897	152662	3177399	26650227	59823925	35385440	4881785	61851
	0.0007%	**0.1173%**	**2.4416%**	**20.4790%**	**45.9710%**	**27.1915%**	**3.7513%**	**0.0475%**
N[0.5, 0.75)	255	38374	627733	4235769	11121962	10632349	2638530	65056
	0.0009%	**0.1307%**	**2.1381%**	**14.4270%**	**37.8813%**	**36.2137%**	**8.9868%**	**0.2216%**
N[0.75, 1)	4	905	30043	196838	611727	895235	432303	30042
	0.0002%	**0.0412%**	**1.3674%**	**8.9590%**	**27.8425%**	**40.7463%**	**19.6761%**	**1.3673%**
Dead	T[−1, −0.75)	T[−0.75, −0.5)	T[−0.5, −0.25)	T[−0.25, 0)	T[0, 0.25)	T[0.25, 0.5)	T[0.5, 0.75)	T[0.75, 1)
N[−1, −0.75)	2157	17975	34195	45471	38048	16498	2191	25
	1.3777%	**11.4812%**	**21.8415%**	**29.0438%**	**24.3025%**	**10.5378%**	**1.3995%**	**0.0160%**
N[−0.75, −0.5)	13472	244397	1112990	2657168	2616850	1030260	129771	1918
	0.1726%	**3.1306%**	**14.2566%**	**34.0365%**	**33.5200%**	**13.1969%**	**1.6623%**	**0.0246%**
N[−0.5, −0.25)	27130	795739	6105060	19946327	22732054	9355171	1238490	19905
	0.0451%	**1.3214%**	**10.1379%**	**33.1225%**	**37.7484%**	**15.5350%**	**2.0566%**	**0.0331%**
N[−0.25, 0)	26559	1184801	10812917	41537423	57090359	27525978	4224644	81291
	0.0186%	**0.8315%**	**7.5889%**	**29.1523%**	**40.0679%**	**19.3186%**	**2.9650%**	**0.0571%**
N[0, 0.25)	17384	1084594	11855469	52334484	8.43E+07	47341213	8402419	196268
	0.0085%	**0.5276%**	**5.7668%**	**25.4570%**	**41.0294%**	**23.0281%**	**4.0872%**	**0.0955%**
N[0.25, 0.5)	7709	586844	7584976	41334942	81234297	53617788	11292281	347076
	0.0039%	**0.2994%**	**3.8698%**	**21.0886%**	**41.4448%**	**27.3552%**	**5.7612%**	**0.1771%**
N[0.5, 0.75)	1510	126824	1643208	9757545	22967367	20208793	6471237	327785
	0.0025%	**0.2062%**	**2.6717%**	**15.8648%**	**37.3427%**	**32.8575%**	**10.5216%**	**0.5329%**
N[0.75, 1)	21	3841	48287	234001	590675	863640	561199	57167
	0.0009%	**0.1628%**	**2.0471%**	**9.9202%**	**25.0410%**	**36.6131%**	**23.7914%**	**2.4235%**

Table 4's top panel is for Alive samples and the bottom panel is for Dead samples of the overlap DM sites' correlation or co-methylation with all 391,459 CG sites. For each correlation level or interval, there are two rows. One row is the count, and the next row is the corresponding percentage. The first column is for normal tissues' correlation intervals (i.e., 'N' means normal). The other eight columns are tumor tissues' correlation intervals (i.e., 'T' means tumor).

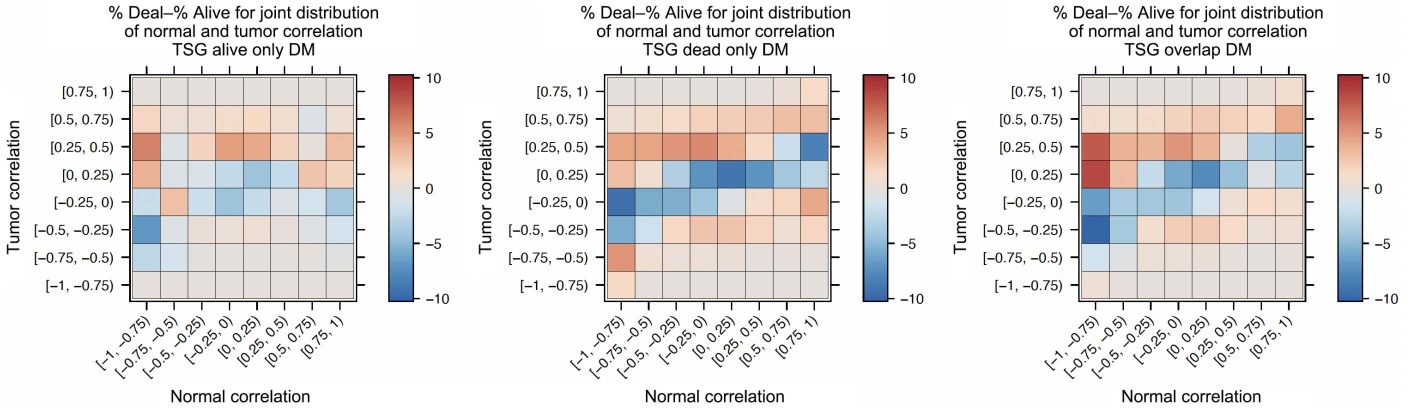

Fig. 6 Heatmaps of comparing co-methylation changes from normal to tumor.

or low correlations tended to remain in the same or nearby intervals, except that some of these were changed to high correlations (see the purple bars on the bottom left plot).

Co-methylation analysis part 3: identifying genes with complex co-methylation changes

To find important genes involved in complex co-methylation changes, the authors identified the genes associated with the CG sites that fell within certain correlation levels (or intervals) shown in the 8 × 8 matrix. This was done for the overlap DM sites in Alive and Dead data separately. A negative to positive CG pair (neg2pos) was defined as one that had a highly negative correlation coefficient in the normal data but a highly positive correlation coefficient in the tumor data. The inverse of that was referred to as a positive to negative (pos2neg) correlation change. A sleeping CG site pair (sleeping.neg or sleeping.pos) was defined as one that had a low or 0 correlation coefficient (i.e., 'sleeping') in the normal data and a

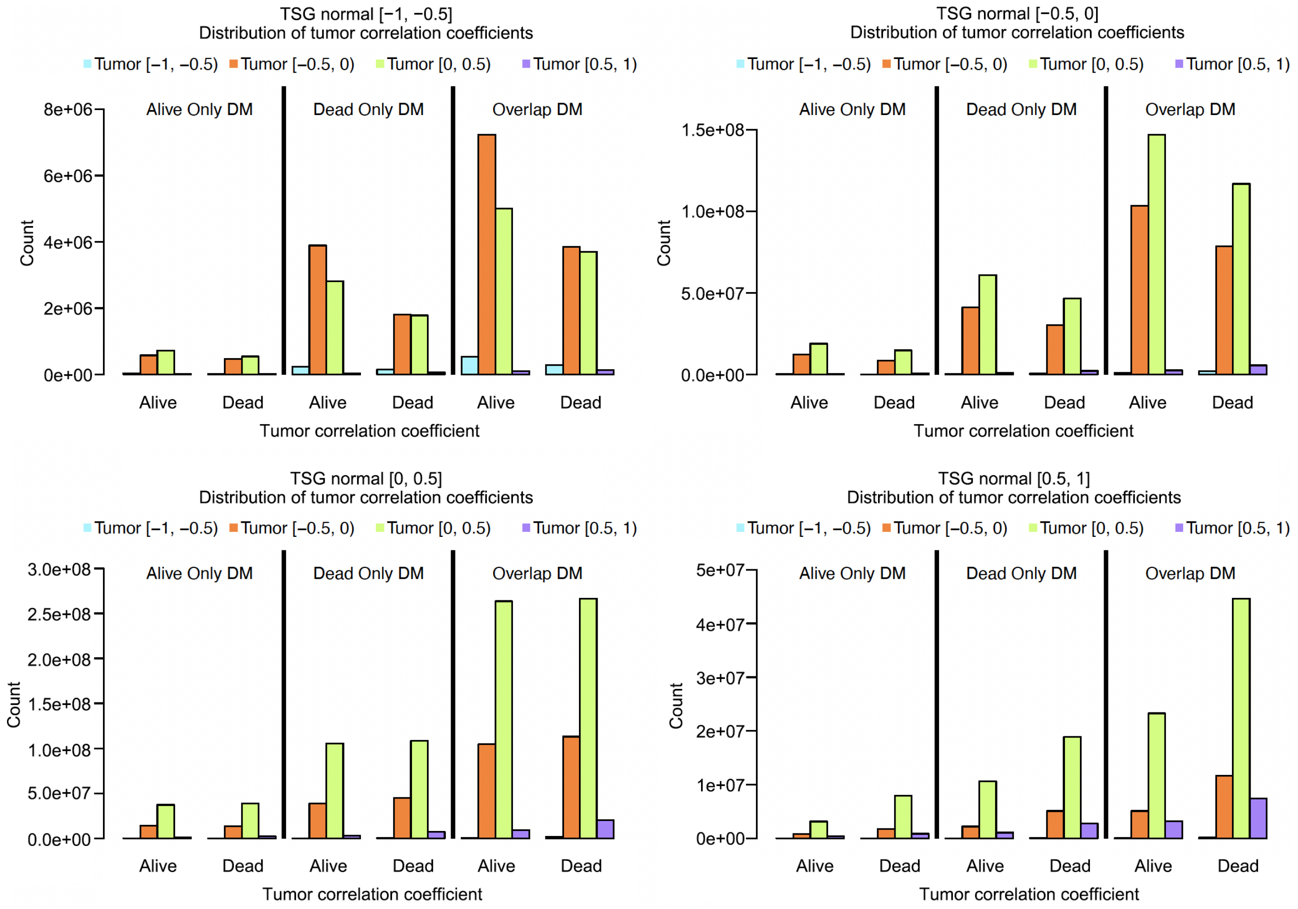

Fig. 7 Comparing the co-methylation changes in Alive and Dead samples based on 4 × 4 matrices.

highly positive or negative correlation coefficient in the tumor data. Similarly, a shutting-down CG site pair (neg2shutting or pos2shutting) was defined as one that had a highly negative or positive correlation coefficient in the normal data but a low correlation coefficient (i.e., 'shutting') in the tumor data. The specific interval criteria and shorthand notation for the six categories were outlined in Table 5. From this point forward, the categories will be referred to as 'panels', and the indicated shorthand will be used.

Gene analyses were further conducted by looking at the CG sites associated with TSGs and non-TSGs separately. All TSGs and non-TSGs associated with CG sites for each correlation (or co-methylation) change were obtained. The number of CG sites per gene in each of the six correlation changes was used to find genes of interest. For each of those six changes/panels listed in Table 5, $N_{g.Alive}$, and $N_{g.Dead}$ were used to denote the numbers of CG sites associated with a gene (g) in Alive and Dead data, respectively. The four selection methods (A, B, C, and D) were listed below. Essentially, the authors separated the data into four categories: TSG overlap-DM Alive data, TSG overlap-DM Dead data, non-TSG overlap-DM Alive data, and non-TSG overlap-DM Dead data.

A. Only-alive for each change/panel: $N_{g.Alive} \geq 3$ and $N_{g.Dead} = 0$.

B. Only-dead for each change/panel: $N_{g.Alive} = 0$ and $N_{g.Dead} \geq 3$.

C. Shared in ≥ 4 same panels: the gene had $N_{g.Alive} \geq 3$ and $N_{g.Dead} \geq 3$ in at least four of six common panels (neg2pos, pos2neg, sleeping.neg, sleeping.pos, neg.shutting, pos.shutting). That is, the authors extracted CG sites that were present in the same ≥ 4 panels between the Alive and Dead samples and were also associated with ≥ 3 CG sites.

D. Difference: $|N_{g.Alive} - N_{g.Dead}| \geq 3$ and both $N_{g.Alive}$ and $N_{g.Dead}$ were not zero in at least four panels (neg2pos, pos2neg, sleeping.neg, sleeping.pos, neg.shutting, pos.shutting). That is, the authors obtained CG sites that were present in ≥ 4 same panels between Alive and Dead samples and had an absolute difference of ≥ 3 CG sites when comparing the respective genes/panels between Alive and Dead datasets.

Table 5. Definition of co-methylation pattern changes from normal to tumor tissues.

Panel	Panel shorthand	Normal interval	Tumor interval
Normal negative to tumor positive	neg2pos	[−1, −0.75)	[0.5, 1)
Normal positive to tumor negative	pos2neg	[0.75, 1)	[−1, −0.5)
Normal sleeping to tumor negative	sleeping.neg	[−0.25, 0.25]	[−1, −0.75)
Normal sleeping to tumor positive	sleeping.pos	[−0.25, 0.25]	[0.75, 1)
Normal negative to tumor shutting	neg.shutting	[−1, −0.75)	[−0.1, 0.1]
Normal positive to tumor sleeping	pos.shutting	[0.75, 1)	[−0.1, 0.1]

Based on the selection methods A and B (i.e., only-alive or only-dead for each panel), genes were further filtered by only extracting those associated with ≥ 3 CG sites in each panel. The selected TSGs and non-TSGs are shown in Table 6. This table shows that Dead samples (2nd and 4th rows) had more genes associated with co-methylation changes than Alive samples (1st and 3rd rows). For the non-TSG panels (see Table 6 last two rows), there was a notable difference between the raw number of extracted genes in the Alive and Dead samples. In five out of six panels (neg2pos, po2neg, sleeping.neg, sleeping.pos, pos.shutting), the Dead samples contained a larger number of genes. Most notably, for the sleeping.pos and pos.shutting panels, Alive data contained 20 and 67 genes, respectively, while Dead data contained 2,288 and 2,193 genes, respectively. In the neg.shutting category, however, Alive samples contained 605 genes while Dead samples contained 100 genes. When looking at the TSGs (see Table 6 first two rows), the neg.shutting genes in the Alive data were similar to the Dead data (20 vs 23). However, there were also more pos.shutting genes in Dead samples than in Alive samples (61 vs 1). Furthermore, when examining genes found in Alive samples for each change, no genes were found in pos2neg and sleeping.pos panels. The neg.shutting panel had the largest number of TSGs (20 genes). Additionally, the sleeping.pos panel had the most genes (81) associated with it in the Dead data.

Based on the selection method C (Alive and Dead shared in ≥ 4 same panels), 33 TSGs and 68 non-TSGs were identified. In the non-TSG data, only EIF2B5 had changes (or were present) in all six panels at high-frequencies. That is, only 1.5% (1/68) of the multiple-panel and high-frequency genes were present in all six panels. In the TSG data, TP73, EPHB3, and MAD1L1 were present in all six panels with high-frequencies. That is, 9% (3/33) of the multiple panel and high-frequency genes were present in all six panels.

Based on the selection method D (Alive and Dead difference), 30 TSGs and 92 non-TSGs were identified. The only gene with changes in all six panels for the TSG dataset was TP73. In the non-TSG dataset, only DIIP2C and EIF2B5 were present in all six panels. In both datasets, the Dead-counts were typically higher than the Alive-counts. The only exceptions to this were pos.shutting counts for the non-TSG DIP2C (difference of −5) and the neg.shutting counts for the non-TSG EIF2B5 (difference of −9).

The above co-methylation analysis shows that multiple CG sites on the same gene can have different and complex co-methylation relationships with other CG sites in the genome. These co-methylation patterns changed between tumor and normal tissues and between Alive and Dead samples (i.e., at different cancer stages). These patterns and changes indicated complex interactions between genes, which might affect tumor growth and thus cancer development. The differences in certain co-methylation changes (e.g., sleeping.pos or pos.shutting) might play an important role in differentiating between Alive and Dead samples and between non-TSGs and TSGs.

Co-methylation analysis part 4: network and pathway analysis

The ConsensusPath Database (CPDB) analysis[19–21] was conducted for the 30 TSG and 92 non-TSG lists identified based on method D. These genes were selected based on |Dead − Alive| ≥ 3 and both were non-zero counts in at least four panels. This analysis was to further investigate how the selected significant genes interacted with others. The CPDB analysis shows different interactions and relationships among the genes from this study and other genes in the genome; see Fig. 8 (based on 30 TSGs) and Fig. 9 (based on 92 non-TSGs).

In the TSG CPDB figure (Fig. 8), TP73, PPP1CA, PAX6, POU6F2, ESR1, TFAP2A, and ZIC1 were notable hub genes (i.e., genes with many interactions). The first five genes mainly had key protein interactions with other genes (see the orange lines). TFAP2A and ZIC1 mainly had gene regulatory interactions with other genes (see the light blue lines). Additionally, most entities were proteins, while a few were genes, and some intermediate nodes were protein complexes. TFAP2A and ZIC1 were extremely interconnected as they shared 6 gene intermediate nodes through gene regulatory interactions (see the right side of Fig. 8). As for the key hub gene ESR1, patients with ESR1 mutant-positive metastases exhibited poor overall survival[22]. PAX6 was also found to be highly expressed in breast cancer tumors and was involved in breast cancer cell proliferation and tumor progression[23]. ZIC1 was found to be negatively correlated with survival. It was an inhibitor of apoptosis in breast cancer. Because it acted as a tumor suppressor, targeting ZIC1's expression might be useful when developing a possible treatment method[24]. TP73-AS1 was upregulated in breast cancer tumors and associated with poorer prognosis[25]. Lastly, PPP1CA might serve as a possible breast cancer biomarker because it plays a prominent role in cancer progression by inhibiting cell proliferation and migration[26].

For the non-TSG CPDB figure (Fig. 9), most entities were proteins and RNAs, while a few were genes. Most of the relationships among these entities were protein interactions (see orange lines). From the 92 gene list, HDAC4, MAGI1, and RPTOR, served as hub genes in this figure. Additionally, q69yn44, HNRNPL, HSPA5, DENND1A, SH3PXD2A, INPP5E, SALM2, and KIF13B were intermediate nodes that served as hub genes, which were not from the 92 non-TSG list. The last five of these genes were in the top left part of this figure. One interesting hub gene is q69yn44, which was not identified by this study, but it had many interactions with other genes. This gene is a protein-coding gene. It is involved in mRNA methylation, mRNA alternative polyadenylation, and RNA binding activity[27,28]. It acted as a key regulator of mammalian mRNA methylation N6-methyladenosine (m6A) methylation. It did so with METTL3 and METTL14, and m6A was linked to mRNA processing and regulates gene expression.

Among these non-TSG hub genes, HNRNPL has been found to affect gene expressions and was related to the occurrence of breast cancer. Silencing of HNRNPL impacted the expression of NSP 5a3a, B23, and reduced interactions with lncRNA[29]. It thus served as an important gene in suppressing tumor invasion. This suggested that HNRNPL could be targeted when looking for breast cancer treatment options. The hypomethylation of CG sites associated with RPTOR in blood was also found to be associated with breast cancer, presenting it as a promising biomarker for breast cancer detection[30]. HDAC4 was also found to play a role in breast cancer growth and invasion[31]. The targeting of HDAC4 could potentially decrease breast cancer cell growth and invasion. MAGI1 was reported as a new potential tumor suppressor gene in estrogen receptor-positive breast cancer[32].

Discussion

To clarify some terms used in the DM analysis results (e.g., 'overlap DM sites' and 'shared genes'), the authors added the following

Table 6. Summary of number of genes with different co-methylation changes.

Category	neg2pos	pos2neg	sleeping.neg	sleeping.pos	neg.shutting	pos.shutting	Total
TSG identified by Method A: only Alive for each change or panel, $N_{g.Alive} \geq 3$ and $N_{g.Dead} = 0$	1	0	2	0	20	1	24
TSG identified by Method B: only Dead for each change or panel, $N_{g.Alive} = 0$ and $N_{g.Dead} \geq 3$	11	17	49	81	23	61	242
Non-TSG identified by Method A: only Alive for each change or panel, $N_{g.Alive} \geq 3$ and $N_{g.Dead} = 0$	4	5	5	20	605	67	706
Non-TSG identified by Method B: only Dead for each change or panel, $N_{g.Alive} = 0$ and $N_{g.Dead} \geq 3$	38	123	601	2,288	100	2,193	5,343

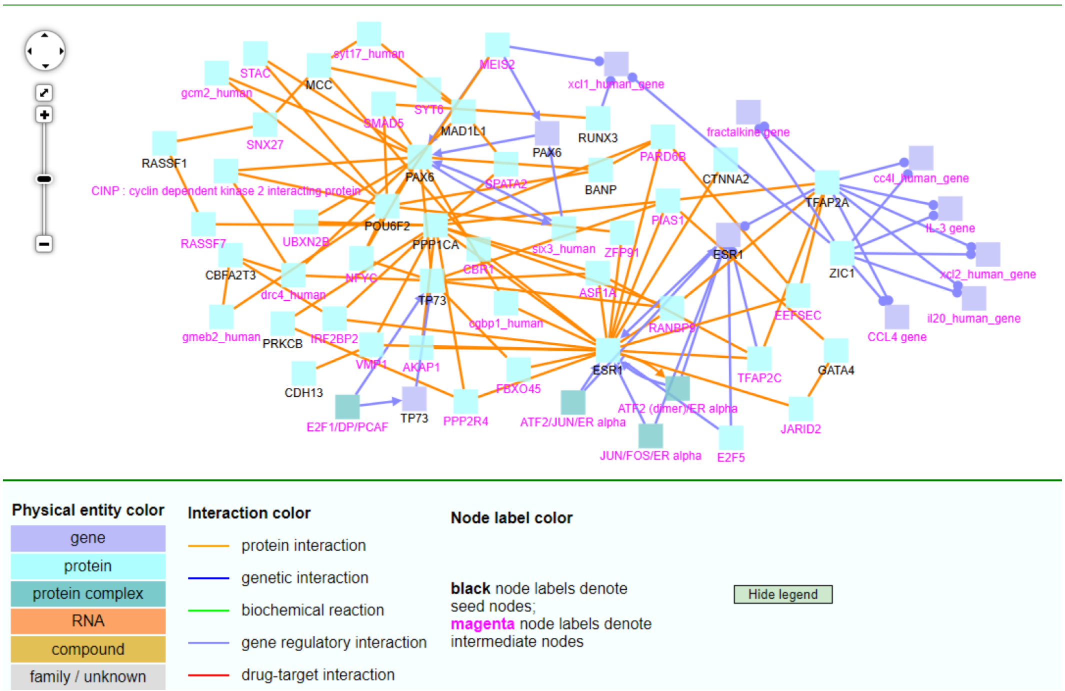

black node labels denote seed nodes; **magenta** node labels denote intermediate nodes

Fig. 8 The CPDB network analysis of 30 TSGs.

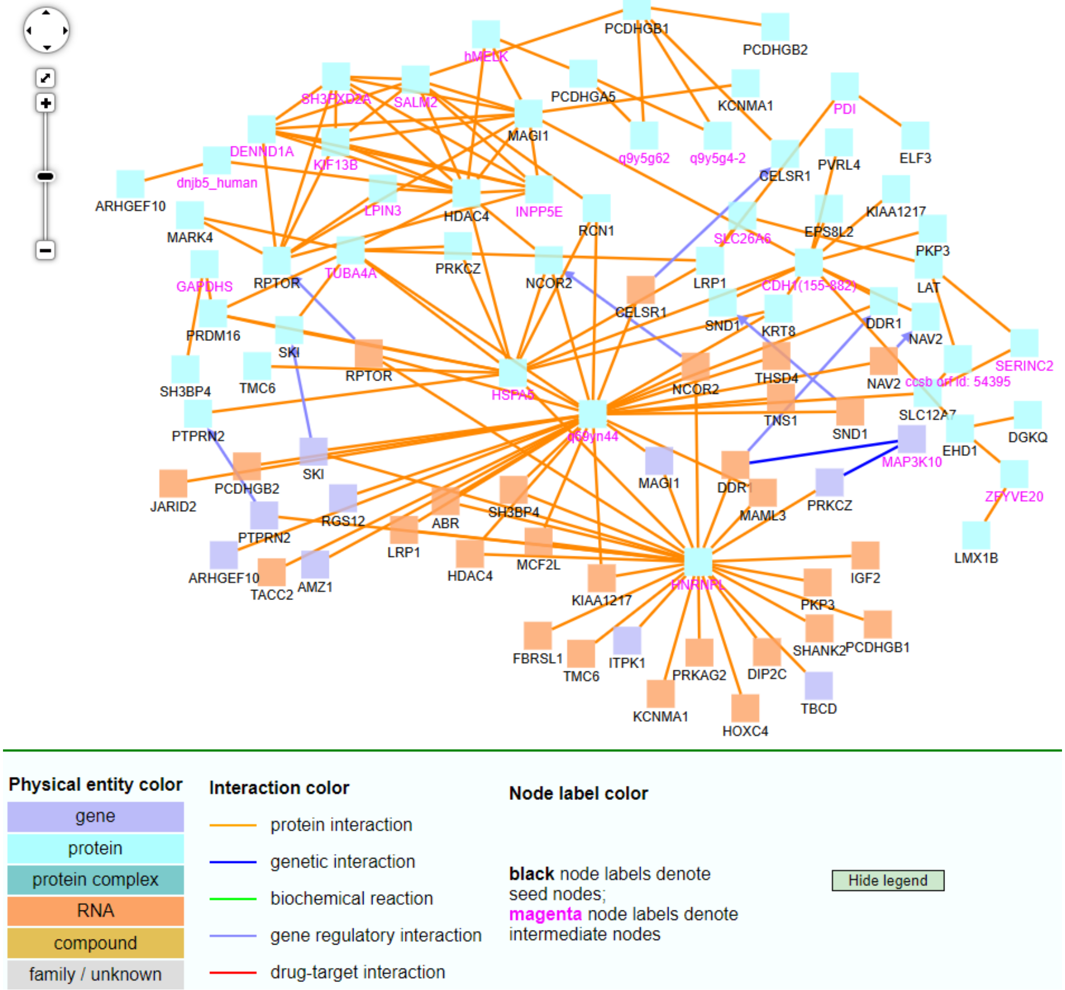

black node labels denote seed nodes; **magenta** node labels denote intermediate nodes

Fig. 9 The CPDB network analysis of 92 non-TSGs.

explanation. First, since a single CG site may be associated with multiple genes, and a gene may consist of multiple CG sites, there are many ways genes can be shared between the three groups: alive-only, dead-only, and overlap (i.e., in both Alive and Dead groups). For example, Fig. 10 shows that CG1 is associated with both Gene A and Gene B, and Gene A covers three CG sites (CG1, CG2, and CG3). Second, 'overlap DM sites' refer to CG sites that were identified as differentially methylated in both Alive and Dead data. For example, Fig. 10 shows that CG3 is an overlap DM site as it is identified in both Alive and Dead samples. However, CG1 and CG2 are not 'overlap DM sites', as they are identified in the alive-only and dead-only respectively. Finally, a shared gene between two groups refers to a gene that has at least one DM site in both groups. For example, Figure 10 shows that CG1 is a DM site for alive-only, and CG2 is a DM site for dead-only, but both CG sites are associated with Gene B, a shared gene between alive-only and dead-only. Additionally, a shared gene among three groups refers to a gene that has at least one DM site in all three groups, e.g., Gene A in Fig. 10.

Pearson's and Spearman's correlations were commonly used. As for which one to use, the authors shared some input. First, when calculating the correlation between CG sites, both Pearson and Spearman methods reached similar conclusions for most CG sites. However, Pearson is sensitive to outliers. A single outlier can cause misleading results for a specific CG site regarding the number of CG sites with which this site is highly correlated. Spearman can counteract the impact of these outliers because it ranks the data and applies Pearson's equation to each rank of the data[33]. Second, Spearman is also more suitable for skewed data. When the distribution is heavily skewed or there are outliers, the Spearman method is more reliable than the Pearson method[34]. Third, overall, when using the Pearson correlation, using beta-values or M-values to calculate correlation did not appear to have a significant difference regarding the main conclusions on the overall co-methylation patterns. However, beta-values appeared to produce slightly high correlations for a small number of CG sites. Spearman correlation, as a rank-based metric, is not affected by the logit transformation. That is, using beta-values or M-values will give the same result. Fourth, while the Pearson method is only able to detect linear relationships, the Spearman method can detect linear and non-linear relationships[35,36]. Since both linear and non-linear correlation were important, the Spearman method was selected to calculate correlation coefficients in this study.

Cao and colleagues reported key genes and important DNA methylation regions in breast cancer[37]. They found that 17 TSGs may be breast cancer biomarkers that are regulated by DNA methylation in key regions. These 17 TSGs were then further compared with the TSG and non-TSG gene lists that had important co-methylation patterns as listed in the six panels (see Table 5). Out of their 17 TSGs, six were found in the TSG list of this study, and these genes were PROX1, CAV1, STAT5A, FAT4, PPARG, and ID4. Five of them (except ID4) were on the selected TSG list, and another five of them were on the selected non-TSG list. These genes and their special co-methylation change patterns are listed in Table 7. The identification of six genes in both studies implied that some non-TSGs identified by this study can be TSGs. Although they were not yet listed in the TSGgene 2.0 list[14], it is likely that they were not yet identified or reported as having TSG functions. Of the 10 genes in Table 7, six of them (STAT5A, FAT4, PPARG, KIT, SOX17, and PREX2) were identified as having co-methylation changes in Dead samples but not Alive samples. This finding might indicate that the co-methylation changes of these genes might be associated with breast cancer death. The genes that were first identified by the authors might play an important role in breast cancer development at different stages, and further biological or experimental validations of these genes and findings need to be done.

For the 30 TSGs and 92 non-TSGs, further gene analysis was also conducted using the Database for Annotation, Visualization and Integrated Discovery (DAVID)[38–44]. GO functional and KEGG pathway enrichment analyses were conducted, and categories with *p*-value < 0.05 and gene counts ≥ 5 were selected as being statistically significant. The 30 TSG genes corresponded to 95 DAVID categories, 31 (32.6%) of which were statistically significant. These categories were mainly associated with or enriched in disordered regions, transcription regulations, RNA polymerase II, and nuclei. The 92 non-TSG genes corresponded to 126 total DAVID categories, 51 (40.4%) of which were statistically significant. These categories were mainly associated with or enriched in disordered regions, cytoplasms, plasma membranes, and cadherins. Overall, TSG and non-TSG were associated with different functions or regions, except that both had the highest number of genes associated with disordered regions. This was expected when analyzing breast cancer data.

As for methylation states, Tian et al. used an additional methylation state, 'bimodal', when analyzing breast cancer cell line data[13]. If over 40% of the samples have a methylation level below 0.2 and over 40% of the samples have a methylation level above 0.8, this site is called 'bimodal'. In this study, only a single CG site was classified as 'bimodal', the authors have decided to exclude the bimodal classification to focus on the more significant methylation states. Instead, any CG sites that would have been categorized as bimodal have been classified as 'Rest' (i.e., a heterogeneous state). Note, Tian et al.'s study used methylation sequencing data of breast cancer cell lines, while this study used the Illumina methylation array data of breast cancer patients' primary tissues. That is, the methylation data used in Tian et al.'s study and this study were different, which may explain why it was unnecessary to include a 'bimodal' state in this study.

The Alive and Dead samples were selected using the vital status data directly provided by the TCGA. Using the TCGA web portal, the authors selected available DNA methylation data for breast cancer samples, which provided a total of 1,095 datasets at the time they obtained the data (892 Illumina 450 K, 342 Illumina 27 K, and some patients or samples have both 450 and 27 K data). The authors

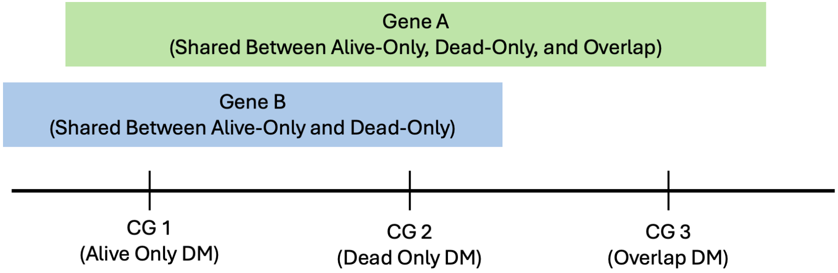
Gene A
(Shared Between Alive-Only, Dead-Only, and Overlap)
Gene B
(Shared Between Alive-Only and Dead-Only)
CG 1
(Alive Only DM)
CG 2
(Dead Only DM)
CG 3
(Overlap DM)

Fig. 10 Visualization or example of overlap DM sites and shared genes.

Table 7. Genes identified by both this study and a previous study.

Category	Gene	Samples (Alive/Dead), co-methylation change/panel
TSG	PROX1	Alive and Dead, shared in ≥ 4 same panels
TSG	CAV1	Alive, neg.shutting
TSG	STAT5A	Dead, pos2neg
TSG	FAT4	Dead, sleeping.pos and neg.shutting
TSG	PPARG	Dead, sleeping.pos
Non-TSG	PRDM16	Alive and Dead difference
Non-TSG	RYR3	Alive, neg.shutting
Non-TSG	KIT	Dead, sleeping.pos
Non-TSG	SOX17	Dead, sleeping.pos
Non-TSG	PREX2	Dead, pos.shutting

The first column is the category, i.e., TSG or non-TSG, based on the TSG database used in this study. The second column consists of gene names identified by both this study and Cao et al.[37]. The third column shows in which sample and with which co-methylation change pattern (or panel) each gene was identified.

specifically focused on (a) female patients, (b) samples with Illumina methylation 450 K array data, (c) only samples with matched normal tissue available, and (d) samples with vital status provided. These criteria left the authors with 53 Alive samples and 32 Dead samples, as there were only a small number of patients with matched normal tissues. The authors intentionally chose to use the BRCA patients with matched normal (or paired) data for the following reasons as reported in the literature. First, a paired design with tumors and adjacent normal tissues from the same patient reduces variability and improves the efficiency of identifying differentially expressed genes[45]. Second, using the paired design identified different genes than using the tumor with normal tissues from different patients. Stevens et al. found that the statistical power increased as the proportion of paired samples increased[46]. Third, by only focusing on matched samples, researchers can mitigate the impact patient-to-patient variation may have on the results in detecting somatic mutations. For example, using matched normal samples allowed subtraction of the germline variants shared by all cells in an individual, leaving only acquired somatic mutations[47].

Other factors might affect patients' vital status and the DNA methylation profile. These factors may include age at diagnosis, hormone receptor, tumor stage, treatment modality, and tumor histologic type. These factors may be associated with the differences and patterns that were reported in this paper. For example, the Alive group was generally younger than the Dead group (average ages are 53 for Alive and 64 for Dead samples). There were more patients with estrogen-receptor-positive (ER+) and progesterone-receptor-positive (PR+) in the Alive group than in the Dead group (ER+: 73.1% for Alive and 65.6% for Dead; PR+: 62.3% for Alive and 56.3% for Dead). It is very important to incorporate this information. The authors have been working on a methylation-age estimation project that accounts for the above factors. They also plan to conduct future research on co-methylation using other independent datasets and by building new statistical models that incorporate these factors.

Below is a brief comparison between a previous breast cancer co-methylation paper by Sun et al.[17] and this study. First, in the previous 2022 co-methylation paper, the authors investigated the overall co-methylation patterns in the whole genome using all available CG sites. However, in this study, the focus was TSG sites. Second, in the previous 2022 paper, general co-methylation patterns among all CG sites were studied. However, in this study, the co-methylation patterns were analyzed with a focus on the correlation between each DM site and all available CG sites. That is, the purpose of this study was to investigate the impact of differential methylation on co-methylation. Thus, this new project is a more focused study. Third, in the previous 2022 paper, there was no thorough investigation on the co-methylation changes as the authors did in this study. Therefore, one novel aspect of this study is that complex co-methylation changes were analyzed, and associated TSGs and non-TSGs were identified. This study is important because TSGs play a crucial role in the regulation of breast cancer development. Because TSG sites behave differently from other CG sites, analyzing all CG sites together could nullify some important methylation patterns of TSG sites. By focusing on TSGs, the authors of this study have been able to identify more specific methylation patterns and relevant genes as reported in this paper.

As for the DM identification, because the majority of CG sites in the Illumina methylation microarray data are relatively far away from each other (compared with bisulfite sequencing data), it is not necessary to consider the similarity or spatial correlation of nearby CG sites as many other methods did (e.g., hidden-Markov-model-based methods[48,49]). Instead, the authors chose to use simple paired T-tests and then use $p < 0.05$ and beta |mean.difference| ≥ 0.2 to identify certain sites with both statistical and biological significance. The purpose of this study was not to identify an accurate number of DM CG sites. Instead, it was to identify some CG sites with relatively or reasonably large DM signals and then see how their overall co-methylation patterns change genome-wide. The simple method used in this study identified a list of sites with certain DM signals for downstream analysis, and it had an easy and simple biological interpretation.

To further understand Alive and Dead tumors' methylation changes, the authors also compared their methylation states, see Table 8. This table shows the following findings: First, most CG sites had the same methylation state between Alive and Dead (see the diagonal numbers, 59%–88%). None of the CG sites changed to a completely different methylation state, such as L to H or H to L. However, some CG sites changed to a similar methylation state, such as L to LM. Second, very few CG sites with L and H states in the Alive tumor dataset became heterogeneous (R) in the Dead tumor dataset (only 1.27% for L states and 1.21% for H states). But a large percentage of CG sites with LM, M, and HM methylation states changed to R (i.e., a heterogenous state) in the Dead samples (22.68% for LM, 36.07% for M, and 15.92% for HM). This change indicated that the methylation states of these CG sites (L, LM, and HM) in the Alive group became more heterogeneous in Dead samples.

Table 8. Methylation state changes from Alive-Tumor to Dead-Tumor.

	DT_L	DT_LM	DT_M	DT_HM	DT_H	DT_R	Sum
AT_L	67766 (88.06%)	8213 (10.67%)	0 (0%)	0 (0%)	0 (0%)	975 (1.27%)	76954 (100%)
AT_LM	6647 (15.5%)	26287 (61.32%)	214 (0.5%)	0 (0%)	0 (0%)	9723 (22.68%)	42871 (100%)
AT_M	0 (0%)	177 (3.18%)	3291 (59.2%)	86 (1.55%)	0 (0%)	2005 (36.07%)	5559 (100%)
AT_HM	0 (0%)	0 (0%)	364 (0.47%)	55797 (72.57%)	8491 (11.04%)	12240 (15.92%)	76892 (100%)
AT_H	0 (0%)	0 (0%)	0 (0%)	7825 (25.72%)	22228 (73.07%)	367 (1.21%)	30420 (100%)
AT_R	522 (0.33%)	6911 (4.35%)	3201 (2.02%)	17205 (10.84%)	539 (0.34%)	130385 (82.13%)	158763 (100%)
Sum	74935 (19.14%)	41588 (10.62%)	7070 (1.81%)	80913 (20.67%)	31258 (7.98%)	155695 (39.77%)	391459 (100%)

In the first column, 'AT' stands for Alive-Tumor. For example, 'AT_L' means Alive Tumor samples' L methylation state. On the top/first row, 'DT' stands for Dead-Tumor.

For the CG sites shown in the seventh column of Table 8, they changed to a heterogeneous methylation state (R) in the Dead tumor data. The authors then studied their locations based on the feature type (or location) information provided by the Illumina 450K protocol (see Table 9). More than half of the CG sites with L and LM methylation states were located on CpG islands. That is, for CG sites with L states, 75.18% of them were located within CpG islands, and 52.25% of LM CG sites were also found within CpG islands. This is in stark contrast with the fact that only 13.58%–25.89% of H, HM, and M CG sites were in CpG islands. For CG sites with all other methylation states, open-sea was the most common location. In particular, 34.81%–50.59% of CG sites with H, HM, and M methylation states were located in the open-sea, whereas only 6.15% and 15.66% of CG sites with H and HM methylation states were located in the open-sea. The shelf and open-sea regions became more frequent as the methylation state increased from L to H. The R (heterogenous) state had a feature type distribution similar to the M methylation state.

For the CG sites that changed from L, LM, M, HM, and H in Alive-Tumor to R in Dead samples (i.e., the 7th column in Table 8), the authors analyzed how many genes these CG sites were associated with (see Table 10). Only several small percentages of CG sites were not associated with any genes (i.e., associated with 0 genes), ranging from 4.92% for L to 18.05% for HM states (see the 2nd column of Table 10). 57.33% to 79.02% CG sites were associated with one gene (see the 3rd column), and 12.53%–37.74% CG sites were associated with two or more genes (see the 4th column). For CG sites associated with two or more genes, their methylation (or co-methylation) pattern changes were likely to have a more significant impact. To further study this impact, the authors analyzed the CG sites associated with just one gene to see how many isoforms these genes had. Analysis results show that a large percentage of them had two or more isoforms (see columns three through six of Table 11). The fact that these genes had many isoforms might suggest that these CG sites were involving promoter usage and alternative splicing significantly. For the associated genes with five to 10 or more isoforms, the impact could be very complex as different BRCA patients might respond to cancer very differently. Without experimental validation in a wet lab, it is challenging to know their specific impact on carcinogenesis or tumor development. However, these patterns can help researchers have new understandings regarding the functions of DNA methylation.

Conclusions

In this paper, the authors have conducted the first-ever comprehensive analysis of different methylation patterns for 1,217 TSGs using publicly available breast cancer data. The data included methylation signals of tumors and matched normal tissues in 53-Alive and 32-Dead samples. The patterns analyzed in this paper were methylation distribution, differential methylation, and co-methylation. The analysis results show that when comparing tumors with normal tissues for both Alive and Dead samples, there were significantly more DM sites in the Dead group. Many CG sites were DM in both Alive and Dead samples. These DM CG sites tended to be associated with genes that have many CG sites. From normal to tumor tissues, the changes in co-methylation patterns were complex in both Alive and Dead samples. For example, CG sites of one tumor suppressor gene can have several co-methylation changes, and these changes can have different directions. The authors have identified the CG sites and related TSGs and non-TSGs with these significant changes. The top TSGs identified in this study played a key role as hub genes in different networks and pathways. There were more genes involved in the complex co-methylation changes in Dead than in Alive samples. This difference suggests that differential methylation and co-methylation may play a significant role in tumor growth at different cancer stages. The comprehensive

Table 9. Analysis of locations for CGs whose methylation states changed to R in Dead samples.

Alive methy.state	North Shore	South Shore	Open-Sea	Island	South Shelf	North Shelf	Sum
L	94 (9.64%)	86 (8.82%)	60 (6.15%)	733 (75.18%)	2 (0.21%)	0 (0%)	975 (100%)
LM	1435 (14.76%)	1429 (14.7%)	1523 (15.66%)	5080 (52.25%)	134 (1.38%)	122 (1.25%)	9723 (100%)
M	291 (14.51%)	280 (13.97%)	698 (34.81%)	519 (25.89%)	93 (4.64%)	124 (6.18%)	2005 (100%)
HM	1419 (11.59%)	1257 (10.27%)	6192 (50.59%)	1662 (13.58%)	863 (7.05%)	847 (6.92%)	12240 (100%)
H	32 (8.72%)	20 (5.45%)	188 (51.23%)	63 (17.17%)	31 (8.45%)	33 (8.99%)	367 (100%)
R	17577 (13.48%)	16096 (12.34%)	53099 (40.72%)	33522 (25.71%)	5005 (3.84%)	5086 (3.9%)	130385 (100%)

Table 10. Numbers of genes associated with CGs whose methylation states changed to R in Dead samples.

Alive. methy. state	Num_CG_w_0_Gene	Num_CG_w_1_Gene	Num_CG_w_GE2_Gene	Total_Num_CG
L	48 (4.92%)	559 (57.33%)	368 (37.74%)	975 (100%)
LM	944 (9.71%)	6121 (62.95%)	2658 (27.34%)	9723 (100%)
M	340 (16.96%)	1301 (64.89%)	364 (18.15%)	2005 (100%)
HM	2209 (18.05%)	8153 (66.61%)	1878 (15.34%)	12240 (100%)
H	31 (8.45%)	290 (79.02%)	46 (12.53%)	367 (100%)
R	24987 (19.16%)	80592 (61.81%)	24806 (19.03%)	130385 (100%)

Table 11. Numbers of isoforms for CG sites associated with one gene.

Alive_State	1 isoform	2 ~ 4 isoforms	5 ~10 isoforms	11 ~ 20 isoforms	≥ 21 isoforms	Total
L	90 (16.1%)	228 (40.79%)	206 (36.85%)	34 (6.08%)	1 (0.18%)	559
LM	1292 (21.11%)	2667 (43.57%)	1723 (28.15%)	379 (6.19%)	60 (0.98%)	6121
M	322 (24.75%)	539 (41.43%)	350 (26.9%)	80 (6.15%)	10 (0.77%)	1301
HM	1996 (24.48%)	3456 (42.39%)	2149 (26.36%)	490 (6.01%)	62 (0.76%)	8153
H	68 (23.45%)	118 (40.69%)	88 (30.34%)	15 (5.17%)	1 (0.34%)	290
R	20933 (25.97%)	34751 (43.12%)	20118 (24.96%)	4169 (5.17%)	621 (0.77%)	80592

analysis of various methylation patterns of TSG CG sites can help researchers to have a new and better understanding of the functions of TSGs and their interactions with other genes. It may thus pave the way to identify novel TSGs and potential biomarkers to enhance breast cancer studies.

Ethical statements

The datasets used in this study were collected and provided by The Cancer Genome Atlas (TCGA). They are publicly available. Therefore, no ethics committee approval was required for this study. The TCGA web page is www.cancer.gov/ccg/research/genome-sequencing/tcga.

Author contributions

The authors confirm their contributions to the paper as follows: study conception and design: Sun S; data collection: Sun S; analysis and interpretation of results: Pritchard A, Tian C, McFall E, Sun S; draft manuscript preparation: Sun S, Pritchard A, Tian C. All authors contributed their expertise and edits. All authors have read and approved the final manuscript.

Data availability

The original or raw datasets supporting the conclusions of this article are publicly available in the TCGA repository https://portal.gdc.cancer.gov/. The datasets (tables and figures) supporting the conclusions of this article are included within the article. All key TSGs and non-TSGs identified in this study and the corresponding R code files (scripts) that generated these genes can be found on the following web page: https://github.com/ss355/TSG.study.

Acknowledgments

This research was partially supported by two NSF-REU grants: DMS-1757233 and DMS-2150205. This project was also supported by the Texas State University Research Enhancement Program (an internal grant for Dr. Sun). The funders did not play any role in the study design, data analysis, interpretation of data, writing the manuscript, or decision to publish. This project was made possible with the use of Texas State University's facilities and resources. The authors are particularly grateful for the help and support from the colleagues at the High-Performance Computing Cluster and the Writing Center. The authors also appreciate the editor and the two reviewers' thoughtful comments and suggestions, which have helped to improve this paper greatly.

Conflict of interest

The authors declare that they have no conflict of interest.

Dates

Received 16 October 2024; Revised 22 February 2025; Accepted 19 March 2025; Published online 14 April 2025

References

1. Giaquinto AN, Sung H, Miller KD, Kramer JL, Newman LA, et al. 2022. Breast cancer statistics, 2022. *CA: A Cancer Journal for Clinicians* 72:524−41
2. Van De Voorde L, Speeckaert R, Van Gestel D, Bracke M, De Neve W, et al. 2012. DNA methylation-based biomarkers in serum of patients with breast cancer. *Mutation Research* 751:304−25
3. Akulenko R, Helms V. 2013. DNA co-methylation analysis suggests novel functional associations between gene pairs in breast cancer samples. *Human Molecular Genetics* 22:3016−22
4. Zhang J, Huang K. 2017. Pan-cancer analysis of frequent DNA co-methylation patterns reveals consistent epigenetic landscape changes in multiple cancers. *BMC Genomics* 18:1045
5. Sun W, Yang J. 2010. Functional mechanisms for human tumor suppressors. *Journal of Cancer* 1:136−40
6. Yang X, Yan L, Davidson NE. 2001. DNA methylation in breast cancer. *Endocrine-Related Cancer* 8:115−27
7. Wang LH, Wu CF, Rajasekaran N, Shin YK. 2018. Loss of tumor suppressor gene function in human cancer: an overview. *Cellular Physiology and Biochemistry* 51:2647−93
8. Arslan S, Dogan T, Koksal B, Yildirim ME, Gumus C, et al. 2008. Tumoral tissue specific promoter hypermethylation of distinct tumor suppressor genes in a case with nonsmall cell lung carcinoma: a case report. *Lung India* 25:148−51
9. Cul'bová M, Lasabová Z, Stanclová A, Tilandyová P, Zúbor P, et al. 2011. Methylation of selected tumor-supressor genes in benign and malignant ovarian tumors. *Ceska Gynekologie* 76:274−79
10. Tawe L, Grover S, Zetola N, Robertson ES, Gaseitsiwe S, et al. 2021. Promoter hypermethylation analysis of host genes in cervical cancer patients with and without human immunodeficiency virus in Botswana. *Frontiers in Oncology* 11:560296
11. Wang LQ, Chim CS. 2015. DNA methylation of tumor-suppressor miRNA genes in chronic lymphocytic leukemia. *Epigenomics* 7:461−73
12. TCGA GDC Data Portal. n.d. https://portal.gdc.cancer.gov
13. Tian S, Bertelsmann K, Yu L, Sun S. 2016. DNA methylation heterogeneity patterns in breast cancer cell lines. *Cancer Informatics* 15:1−9
14. Zhao M, Kim P, Mitra R, Zhao J, Zhao Z. 2016. TSGene 2.0: an updated literature-based knowledgebase for tumor suppressor genes. *Nucleic Acids Research* 44:D1023−D1031
15. Eisenberg E, Levanon EY. 2013. Human housekeeping genes, revisited. *Trends in Genetics* 29:569−74
16. Du P, Zhang X, Huang CC, Jafari N, Kibbe WA, et al. 2010. Comparison of Beta-value and M-value methods for quantifying methylation levels by microarray analysis. *BMC Bioinformatics* 11:587
17. Sun S, Dammann J, Lai P, Tian C. 2022. Thorough statistical analyses of breast cancer co-methylation patterns. *BMC Genomic Data* 23:29
18. Tang G, Pan H, Xu L, Feng R, Jiang Y, et al. 2019. A comparison of co-methylation relationships between rheumatoid arthritis and Parkinson's disease. *Frontiers in Neuroscience* 12:1001
19. Kamburov A, Pentchev K, Galicka H, Wierling C, Lehrach H, et al. 2011. ConsensusPathDB: toward a more complete picture of cell biology. *Nucleic Acids Research* 39:D712−D717
20. Kamburov A, Stelzl U, Lehrach H, Herwig R. 2013. The ConsensusPathDB interaction database: 2013 update. *Nucleic Acids Research* 41:D793−D800
21. Kamburov A, Wierling C, Lehrach H, Herwig R. 2009. ConsensusPathDB — a database for integrating human functional interaction networks. *Nucleic Acids Research* 37:D623−D628
22. Dustin D, Gu G, Fuqua SAW. 2019. *ESR1* mutations in breast cancer. *Cancer* 125:3714−28
23. Xia X, Yin W, Zhang X, Yu X, Wang C, et al. 2015. PAX6 overexpression is associated with the poor prognosis of invasive ductal breast cancer. *Oncology Letters* 10:1501−6
24. Han W, Cao F, Gao XJ, Wang HB, Chen F, et al. 2018. ZIC1 acts a tumor suppressor in breast cancer by targeting survivin. *International Journal of Oncology* 53:937−48
25. Yao J, Xu F, Zhang D, Yi W, Chen X, et al. 2018. TP73-AS1 promotes breast cancer cell proliferation through miR-200a-mediated TFAM inhibition. *Journal of Cellular Biochemistry* 119:680−90
26. Xie W, Sun Y, Zeng Y, Hu L, Zhi J, et al. 2022. Comprehensive analysis of PPPCs family reveals the clinical significance of PPP1CA and PPP4C in breast cancer. *Bioengineered* 13:190−205
27. Schwartz S, Mumbach MR, Jovanovic M, Wang T, Maciag K, et al. 2014. Perturbation of m^{6}A writers reveals two distinct classes of mRNA methylation at internal and 5' sites. *Cell Reports* 8:284−96
28. Yue Y, Liu J, Cui X, Cao J, Luo G, et al. 2018. VIRMA mediates preferential m^{6}A mRNA methylation in 3'UTR and near stop codon and associates with alternative polyadenylation. *Cell Discovery* 4:10

29. Gu J, Chen Z, Chen X, Wang Z. 2020. Heterogeneous nuclear ribonucleoprotein (hnRNPL) in cancer. *Clinica Chimica Acta* 507:286−94
30. Tang Q, Holland-Letz T, Slynko A, Cuk K, Marme F, et al. 2016. DNA methylation array analysis identifies breast cancer associated RPTOR, MGRN1 and RAPSN hypomethylation in peripheral blood DNA. *Oncotarget* 7:64191−202
31. Hsieh TH, Hsu CY, Tsai CF, Long CY, Chai CY, et al. 2015. miR-125a-5p is a prognostic biomarker that targets HDAC4 to suppress breast tumorigenesis. *Oncotarget* 6:494−509
32. Alday-Parejo B, Richard F, Wörthmüller J, Rau T, Galván JA, et al. 2020. MAGI1, a new potential tumor suppressor gene in estrogen receptor positive breast cancer. *Cancers* 12:223
33. Rousselet GA, Pernet CR. 2012. Improving standards in brain-behavior correlation analyses. *Frontiers in Human Neuroscience* 6:119
34. de Winter JCF, Gosling SD, Potter J. 2016. Comparing the Pearson and Spearman correlation coefficients across distributions and sample sizes: a tutorial using simulations and empirical data. *Psychological Methods* 21:273−90
35. Puth MT, Neuhäuser M, Ruxton GD. 2014. Effective use of Pearson's product-moment correlation coefficient. *Animal Behaviour* 93:183−89
36. Puth MT, Neuhäuser M, Ruxton GD. 2015. Effective use of Spearman's and Kendall's correlation coefficients for association between two measured traits. *Animal Behaviour* 102:77−84
37. Cao YN, Li QZ, Liu YX, Jin W, Hou R. 2022. Discovering the key genes and important DNA methylation regions in breast cancer. *Hereditas* 159:7
38. Dennis G, Jr., Sherman BT, Hosack DA, Yang J, Gao W, et al. 2003. DAVID: database for annotation, visualization, and integrated discovery. *Genome Biology* 4:P3
39. Huang DW, Sherman BT, Stephens R, Baseler MW, Lane HC, Lempicki RA. 2008. DAVID gene ID conversion tool. *Bioinformation* 2:428−30
40. Huang DW, Sherman BT, Tan Q, Collins JR, Alvord WG, et al. 2007. The DAVID gene functional classification tool: a novel biological module-centric algorithm to functionally analyze large gene lists. *Genome Biology* 8:R183
41. Huang DW, Sherman BT, Tan Q, Kir J, Liu D, et al. 2007. DAVID Bioinformatics Resources: expanded annotation database and novel algorithms to better extract biology from large gene lists. *Nucleic Acids Research* 35:W169−W175
42. Jiao X, Sherman BT, Huang DW, Stephens R, Baseler MW, et al. 2012. DAVID-WS: a stateful web service to facilitate gene/protein list analysis. *Bioinformatics* 28:1805−6
43. Sherman BT, Hao M, Qiu J, Jiao X, Baseler MW, et al. 2022. DAVID: a web server for functional enrichment analysis and functional annotation of gene lists (2021 update). *Nucleic Acids Research* 50:W216−W221
44. Sherman BT, Huang DW, Tan Q, Guo Y, Bour S, et al. 2007. DAVID Knowledgebase: a gene-centered database integrating heterogeneous gene annotation resources to facilitate high-throughput gene functional analysis. *BMC Bioinformatics* 8:426
45. Haney S, Kam M, Hrebien L. 2008. Benefits of Using Paired Controls for Analyzing Gene Expression of Prostate Cancer. *2008 8th IEEE International Conference on BioInformatics and BioEngineering, Athens, Greece, 8−10 October 2008*. USA: IEEE. doi: 10.1109/BIBE.2008.4696742
46. Stevens JR, Herrick JS, Wolff RK, Slattery ML. 2018. Power in pairs: assessing the statistical value of paired samples in tests for differential expression. *BMC Genomics* 19:953
47. Teer JK, Zhang Y, Chen L, Welsh EA, Douglas Cress W, et al. 2017. Evaluating somatic tumor mutation detection without matched normal samples. *Human Genomics* 11:22
48. Sun S, Yu X. 2016. HMM-Fisher: identifying differential methylation using a hidden Markov model and Fisher's exact test. *Statistical Applications in Genetics and Molecular Biology* 15:55−67
49. Yu X, Sun S. 2016. HMM-DM: identifying differentially methylated regions using a hidden Markov model. *Statistical Applications in Genetics and Molecular Biology* 15:69−81